José Ésio Bessa Ramos Júnior

Condensação- *psi* do DNA: um estudo teórico e experimental

Tese apresentada junto ao Departamento de Física do Instituto de Biociências, Letras e Ciências Exatas -IBILCE- da Universidade Estadual "Júlio de Mesquita Filho", Câmpus de São José do Rio Preto, para a obtenção do título de Doutor em Biofisica Molecular.

Orientador: Prof. Dr João Ruggiero Neto

São José do Rio Preto - SP

2009

Ramos Junior, José Ésio Bessa.
Condensação-psi do DNA : um estudo teórico e experimental / José Ésio Bessa Ramos Junior. - São José do Rio Preto : [s.n.], 2009.
34 f. : 20 il.; 30 cm.

Orientador: João Ruggiero Neto
Tese (doutorado) - Universidade Estadual Paulista, Instituto de Biociências, Letras e Ciências Exatas

1. Biologia molecular. 2. Ácido desoxirribonucleico. 3. Biofísica. 4. Polímeros. 5. Interação DNA - Proteínas. 6. Condensação de DNA. Biofísica molecular. I. Ruggiero Neto, João. II. Universidade Estadual Paulista, Instituto de Biociência, Letras e Ciências Exatas. III. Título.

CDU - 577.2

Resumo

Na presente tese, a condensação-*psi* ("*psi* é a abreviação para a sentença em língua inglêsa "**p**olymer and **s**alt **i**nduced" - condensação induzida por polímero e sal") do DNA é estudada experimentalmente e teoreticamente em diferentes contextos. Experimentos utilizando espectroscopia de dicroísmo circular são realizados para elucidar a influência do peso molecular do polímero flexível na condensação e decondensação reentrante do DNA. O diagrama de fase completo da transição é determinado e comparado com predições teóricas existentes. Um acordo quantitativo completo é encontrado com relação à condensação, mas apenas um acordo qualitativo é obtido com relação à transição reversa devido às aproximações da teoria.

Esse problema teórico é revisitado nesta tese e um modelo teórico menos restritivo é desenvolvido ao longo das linhas originais da teoria das interações de depleção propostas por Asakura e Oosawa. A decondensação reentrante é encontrada em um amplo espectro de concentrações do sal e a dependência da concentração crítica do polímero flexível (PEG_{crit}) com relação ao seu peso molecular para ambas as transições está em acordo qualitativo com os dados experimentais.

É também discutido ao longo desta tese, o sinergismo experimentalmente observado entre as interações de depleção e a complexão de proteínas básicas com o DNA na condensação dessa macromolécula. Experimentos de eletroforese em gel de agarose e espalhamento dinâmico de luz são realizados para esclarecer esse sinergismo e propôr um modelo microscópico para a formação e estabilidade do nucleóide em células procarióticas.

Por fim, é investigada experimentalmente e teoreticamente a influência da topologia do DNA na condensação-*psi*. Os valores do PEG_{crit} são experimentalmente determinadas para a forma super-helicoidal e a forma linear correspondente. Tanto os resultados experimentais quanto as estimativas numéricas indicam uma influência bastante limitada das super-hélices na condensação do DNA. Simulações de Monte Carlo são realizadas para determinar as possíveis modificações conformacionais do DNA com super-hélices induzidas pelo confinamento dessa molécula no interior do condensado. Uma redução no diâmetro das super-hélices é encontrada como sendo mais provável do que uma significante redução da quantidade de super-hélices (medida pelo "writhe") devido às pequenas variações de energia livre relativas envolvidas no primeiro caso.

Abstract

In the present thesis, the DNA ***psi***-condensation is studied both experimental and theoretically in several different contexts. Experiments using circular dichroism spectroscopy were performed in order to elucidate the influence of the flexible polymer's molecular weight on the DNA condensation and reentrant decondensation. The whole phase diagram was determined and compared with theoretical predictions. A full quantitative agreement is found for the condensation transitions; as far the reentrant decondensation transition is concerned, the model does not predict the entire phase diagram due to its assumptions.

This theoretical problem is revisited in this thesis and a less restrictive model is developed along the lines of the original Asakura-Oosawa model for depletion interactions. The DNA reentrant decondensation is found within a wide range of salt concentration and the critical PEG (**p**oly **e**thylene**g**licol) concentrations (PEG_{crit}) dependence on the PEG's degree of polymerization is in qualitative agreement with the experimental data.

We also discuss in this thesis, the synergism found between molecular crowding and the "histone-like" protein binding to DNA molecules in condensing DNA. An agarose gel electrophoresis assay and dynamic light scattering experiments were performed in order to elucidate this synergism and to propose a microscopic model for the formation and stability of the prokaryotic nucleoid.

At last, we investigate both theoretical and experimentally the influence of the DNA topology on the DNA ***psi***-condensation, namely we investigate the role of super-coiling on the polymer induced DNA condensation and compare the PEG_{crit} critical concentrations for the super-coiled DNA as well as for the linearized form. Both experiments and analytical estimatives show that super-coiling has a limited role on the phase separation which accounts for the DNA condensation. Monte Carlo simulations were also done on this system to investigate to what extend the super-coiled conformation is deformed and we found that a decrease in the plectonemic diameter is most likely to occur in order to fit the super-coiled DNA inside the condensed phase rather than a significant super-helical unwinding.

Content

“Chorava porque não tinha sapatos até que viu um homem que não tinha os pés.”

Adágio chinês

O lamento das coisas

Triste, a escutar, pancada por pancada,
A sucessividade dos segundos,
Ouço, em sons subterrâneos, do Orbe oriundos,
O choro da Energia abandonada!

É a dor da Força desaproveitada
- O cantochão dos dínamos profundos,
Que, podendo mover milhões de mundos,
Jazem ainda na estática do nada.

É o soluço da forma ainda imprecisa...
Da transcendência que se não realiza...
Da luz que não chegou a ser lampejo...

E é um suma, o subconsciente aí formidando
Da Natureza que parou, chorando,
No rudimentarismo do Desejo!

Augusto dos Anjos

“Eu e outras poesias”

Acknowledgments

When I started studying DNA condensation 5 years ago, I realized after some time that a huge amount of work had already been done on the subject and so, one hardly would add something new and interesting to the "established knowledge". Over the last 5 years I have learned a lot about DNA condensation, but above all I learned that there is no such thing like "established knowledge". The background of these acknowledgments is concerned with those who had given me the opportunity to change this very basic viewpoint about scientific research which in turn has changed my entire world perspective.

Firstly, before direct my words to those who are directly involved in this journey, I wish to acknowledge my beloved father Ésio Ramos and mother Fátima Ramos for their unconditional support. Their kindness, care and love during my entire life have allowed me to reach this point of my career. Without my father's wise words I just heard in the right moments or without my mother's tenderness and love, I certainly would not be writing these lines. Thank you two for your incommensurable support.

Now I should address my thanks to my supervisor Joao Ruggiero Neto who opened up the doors of biophysics to me and professor Renko de Vries whose guidance over almost my entire PhD has shaped the core of my conception of science.

Professor João, thank you for the opportunity to start my scientific career dealing with polymer physics and particularly for having attracted my attention to the DNA **psi**-condensation issue. This topic has appeared to me as one of the most fruitful and general in biophysics since it invokes at the same time, the physics fundamental principles as well as its possible technical applications for the proper understanding and appreciation of the theme. It is not easy at all to join these two master lines in the same research project. You have given me the opportunity to work on that and even more importantly you have trusted me to accomplish the task.

Professor Renko, your guidance during the last 3 years has to some extend changed, to say the least, my science's view. During one year, living in the Netherlands and working together with you I learned a lot not only about biophysics, but I learned mainly how to handle scientific issues and how to look for the answers in a very peculiar manner: a balanced mixture of basic principles and a fine touch for the correct experimental ingredients in order to portrait the physical reality as sharp and solid as possible. You made me realize that there is no "established knowledge". Your support and help during that whole period (and I had difficult times as a foreigner) are still alive in my memories and still are the core of our friendship. *Reuze bedankt mijn vriend!*

Right beside Renko's support during that time, the adorable memories of Hermann and Will Kort cross suddenly my mind. One year living together with them and sharing so many times the same dinner table is one of the sweetest memories I have kept with me and I won't forget it ever. Your "goed avond" every night Will, still sounds like the loudest welcome I have ever heard.

In one way or another, I am in debt with all friends I made in Wageningen during 2006-2007. My sincere thanks to my room mate Geert Meijer and his parents who really made me feel at home and from whom I got the deepest impression concerning the kindness of the Dutch people. I am sure our friendship is going to last for a long time, something which does not happen very often nowadays even among country men. That is one the ironies of life!

It is always hard to list the people's names that crossed, at some moment, our lives and were important in some way since one may unfairly omit some one. However I will take this chance (I think I must do it) to thank Renate and Saskia with whom I had the first Chinese lunch in The Netherlands and whose sympathy I had the pleasure to enjoy; Marrat and Ilja with whom I enjoyed many times a cup of tea listening to Ilja at the piano; Petya, his kind wife and beautiful little daughter

who showed me some nice spots around Wageningen, Pascal and Luben for their help with the AFM among other lab's stuff. I hope those I have not mentioned forgive me. Perhaps the most fair and honest way to say thanks is to say it right away when one feels it has to be said.

Here in Rio Preto, the story is a bit different but not a lot. My friends and colleagues in the physics department have supported and helped me out several times. To mention two, when Moreira (nicknamed "Sidney") and Leandro rescued me at the Bady Bassit Avenue (by the way, I used to get lost in Wageningen too!) after I left Vila Dionisio and I got back home safely, and when Ronaldinho kindly informed me that the "Tele Sena" manual had been recovered by Martin Macfly in " Back to the Future II " . These are only two out of hundreds of hands I have been given by friends during my stay in Rio Preto. Thank you all for the nice moments we have had together.

My most sincere thanks to Ana with whom I share the place I have lived over the last 4 years and who has supported and cared about me as a sister. Thank you Ana for our talks about so many different points over all these years.

Here again, in order to acknowledge ever body who has entered into my life and make my stay in Rio Preto (far from my family) somewhat less heavy than it could be and helped me to stand the journey, OBRIGADO.

Introduction

Among the different kinds of mixtures which may be either found in nature or synthesized, there are two major groups: the homogeneous mixtures (solutions) and the heterogeneous mixtures (dispersions and suspensions). The essential physical difference between these two groups is the size of the dissolved particles. Solutions usually have dissolved particles whose sizes are of the order of Angstroms ($1Å=10^{-10}\ m$) whereas in dispersion, particles are nanometer to micrometer sized ($1nm=10^{-9}\ m$ and $1\mu m=10^{-6}\ m$).

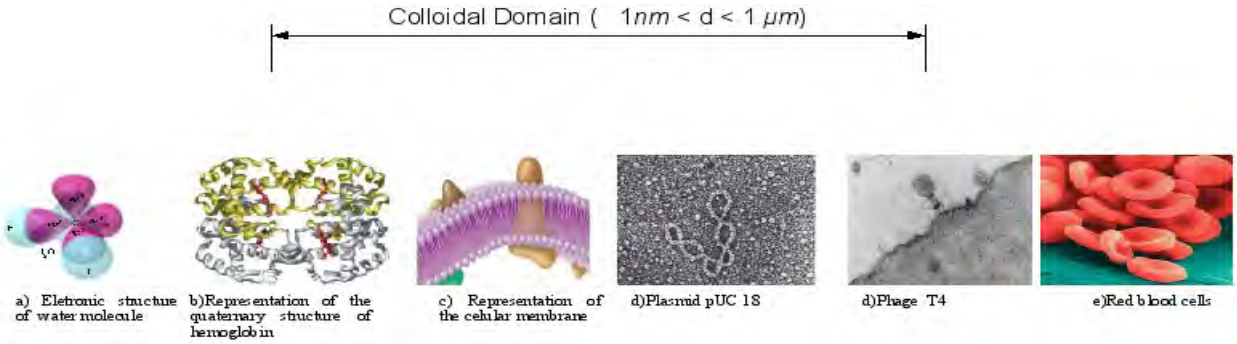

Figure 1- Characteristic length scales of colloidal systems (1nm <d<1 μm): "Colloidal domain" and some biophysical interesting system: a) Illustration of the electronic structure of the water molecule; b) Illustration of the quaternary structure of the hemoglobin molecule. c) Illustration of an eukaryotic plasmatic membrane; d) Electron micrography of the plasmid pUC18; e) Electron micrography of a T4 phage glued to the cell's membrane; f) Electron microscopy of red cells of the human blood.(From "Cellular and Molecular Biology", Lodish,H *et al* .5ª Edition - Artmed Press).

The physical behavior of colloidal dispersions is a direct result of this very basic feature. Due to its sizes, the dispersed particles strongly interact with each other and with external fields in such a way that it is possible to separate them from the dispersant medium by centrifugation or to measure the particles sizes by light scattering which is not strictly possible for solutions (*e.g.*, a dilute solution of sodium chloride (NaCl) dissolved in water (H_2O)) [1].

Bearing these considerations in mind, *the boundaries of the present thesis may be delimited*: the study of dispersions of *neutral and charged polymers*. The phase behavior of these systems is nowadays studied intensively both theoretical and experimentally for technological applications, recent advances in biophysics and medical treatments claim the understanding of those colloidal dispersions [2 and references therein].

The cornerstone of the colloid science was the development of the **DLVO theory** for lyophobic colloids [3] which was worked out in details by **D**eryaguin and **L**andau (Russia) and **V**erwey and **O**verbeek (The Netherlands). The starting point of the DLVO theory is to consider the thermodynamical equilibrium of a colloidal dispersion as a result of the competition between repulsive screened electrostatic interactions and attractive van der Walls interactions among the particles. The former being long-ranged, with a characteristic length given by the Debye length - κ^{-1} which depends on the medium ionic strength- and the later being short-ranged ($\sim r^{-6}$) being r the distance between the particle's centers. Despite the huge amount of work which has been done on colloidal systems and the recent advances in the field, the DLVO theory is still invoked to explain a great number of experimental facts since its publication *in totum* [4].

Another theoretical advance in colloidal systems happened in 1954. Whereas the DLVO theory deals with particles which act on each other *on distance*, Asakura and Oosawa hypothesized that volume restrictions imposed by some dispersed components on others might give rise *to an attractive local potential*. In their famous letter **"On Interactions between two bodies immersed in a solution of macromolecules"**, they pointed out explicitly how this could happen and emphasized the possible implications of these interactions (nowadays called **depletion interactions**) on the phase behavior of colloidal dispersions including some of biological relevance [5].

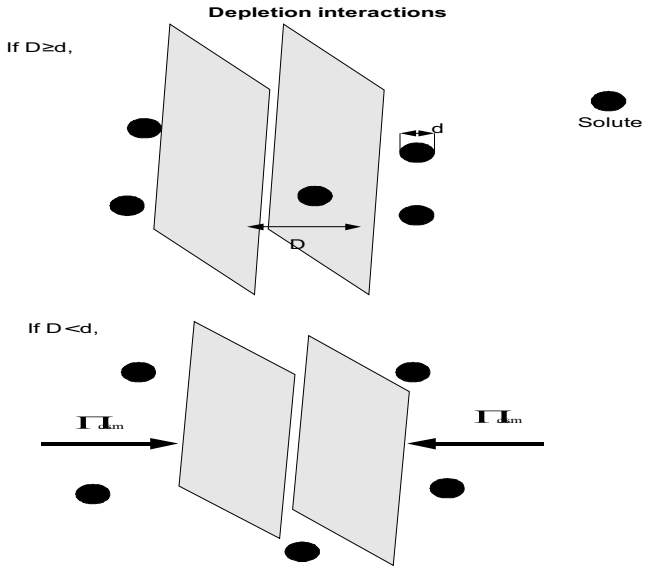

Figure 2- Illustration of the solute depletion from within the inner space between the two parallel surfaces when the distance *D* between the surfaces is smaller than the diameter *d* of the solutes molecules. Once the solute can not enter the space between the plates, the unbalanced osmotic pressure pushes the two plates toward each other.

Ever since this breakthrough, depletion interactions have been invoked to explain a number of experimental facts, and systems which at first glance are uncorrelated such as the crystallization of proteins i*n vitro* [6] and the formation and stability of the prokaryotic nucleoid *in vivo* [7] have been understood on the same theoretical grounds.

When the solutes are modeled as hard spheres (see figure 2) the depletion potential is a discontinuous rather than a smooth function of the distance (*D*) between the interacting surfaces (which were chosen for the sake of clarity as plates) immersed in the dispersion (see figure 3). On the other hand, if the solute molecules are for instance, thin rod-like macromolecules of length *l* or polymer coils of radius of gyration R_g, the depletion potential is a continuous functions of the distance *D* due to the partitioning of the macromolecules between the plates and the bulk of the solution (see figure 3).

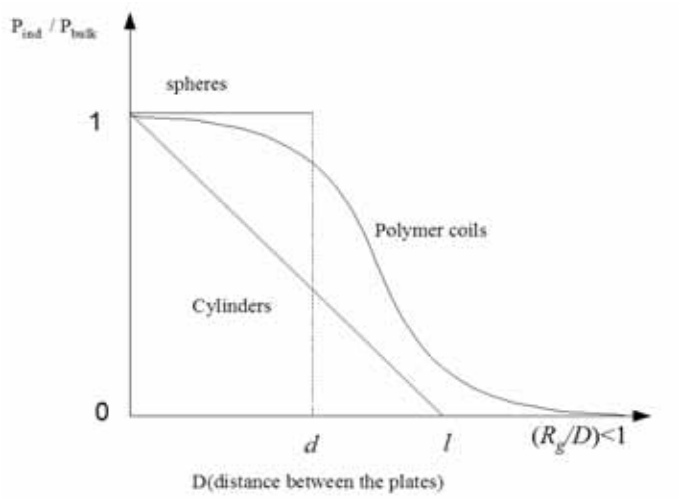

Figure 3 – Illustration of the depletion interactions expressed in terms of the induce pressure P_{ind} (normalized by the solution osmotic pressure P_{bulk} for the case of hard spheres of diameter *d*, thin rod-like macromolecules of length *l* and for polymer coils of radius of gyration R_g as a function of the distance *D* between the plates.

In the figure 4 we illustrate the depletion (exclusion) of the polymer coils from within the space between the surfaces of two plates and from within the space between the surfaces of two spheres. The center of mass of the polymer molecule can not approach the center of the sphere infinitely. Thus there is a depletion layer around each sphere and its radius is nearly $R_{Dep} = R_s + R_g$ where R_{Dep} is the radius of the depletion zone, R_s is the radius of the hard spheres and R_g is the polymer's radius of gyration. When the two hard spheres approach each other and the depletion zones do overlap the polymer molecule is excluded from that space and exert a pressure equals to the solution osmotic pressure and which tends to push the spheres toward each other (see figure 4).

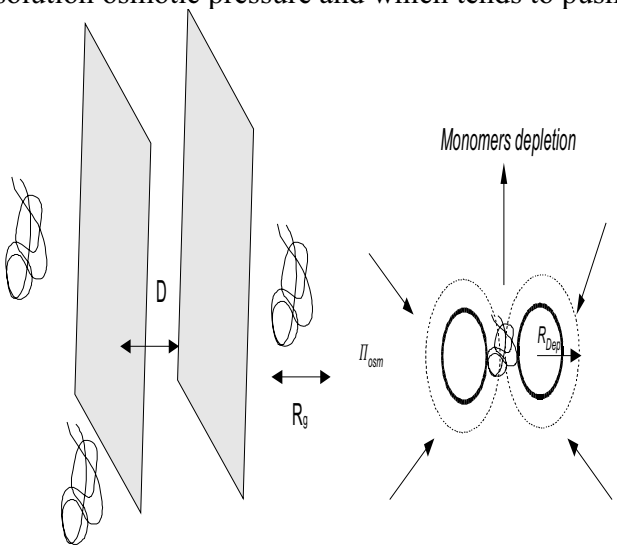

Figure 4- Illustrative picture of polymers coils depleted from within the space between the plates and the spheres surfaces when the depletion layers (represented by dashed circles) do overlap or when R_g is of the order of magnitude of the distance (*D*) between the plates.

Although we have restricted ourselves to the “mechanical effects” of the induced depletion interactions, it has been recognized that these interactions are ubiquitous in the context of physiological processes: the rate of kinetic reactions strongly depends on molecular crowding and so on depletion interactions; the proteins folding and protein stability *in vitro*, the actin polymerization and the formation and stability of the nucleoid in prokaryotic organisms to name a few, do claim the presence of depletion interactions to be rationalized.

The main content of the present thesis deals with *depletion interactions* and its implications on systems of biological relevance emphasizing its importance in some different contexts as well as comparing its significance with the significance of others interactions which ultimately form the scaffold of the current understanding of colloidal systems. More precisely, in the following chapters the phase behavior of mixtures of the poly-electrolyte DNA (***D****eoxyribo****n****ucleic* ***A****cid*) and neutral - flexible polymers will be discussed in several contexts. In what follows, a brief summary of the thesis content is presented along with the main ideas of each paper which form the text’s body. The main purpose of the summary is to allow the reader who has had no previous contact with DNA condensation to gain some insight on the subject without the need of going deep into the subtleties of this wild and rich branch of polymer physics.

Paper 1

Summary

The content of the first paper is concerned with the so-called **p**olymer and **s**alt **i**nduced DNA condensation or ***psi***-condensation (or yet **ψ**-condensation) for the special case in which the depletant is a flexible polymer (**p**oly **e**thylene**g**lycol or PEG) of low molecular weight (2-8*k*). The DNA **ψ**-condensation was discovered by Lerman in 1971[8] and since then, this experimental finding has opened up the doors for an accurate study of the DNA in the liquid-crystalline state: on one hand, it has allowed the experimentalist to accurately measure the intermolecular forces between DNA segments as a function of its distances via X-ray diffraction measurements [9] and thus improve our basic knowledge concerning the statistical-mechanics of tightly confined poly-electrolytes [10,11]; on the other hand, the DNA **ψ**-condensation has stimulated a great deal of theoretical efforts towards the understanding of the underlying physical interactions which govern the phase behavior of flexible/semi-flexible and charged polymers mixtures.

In 1972, Jordan and co-workers performed a series of experiments using circular dichroism spectroscopy (CD) to study the phase behavior of concentrated DNA solutions and discovered an anomalous optical activity at some solutions physicochemical conditions, namely above some critical concentrations of PEG and sodium chloride (NaCl)[12]. Notwithstanding the limitations of the experimental technique (which in general does not allow one to relate *ab initio* the spectrum and the corresponding molecular structure), it was suggested by those authors that the **ψ**-spectra might be the result of the interaction of the circularly polarized light with a molecular aggregate whose supra molecular chirality would be responsible for the anomalous selective absorption of one of the polarized light states.

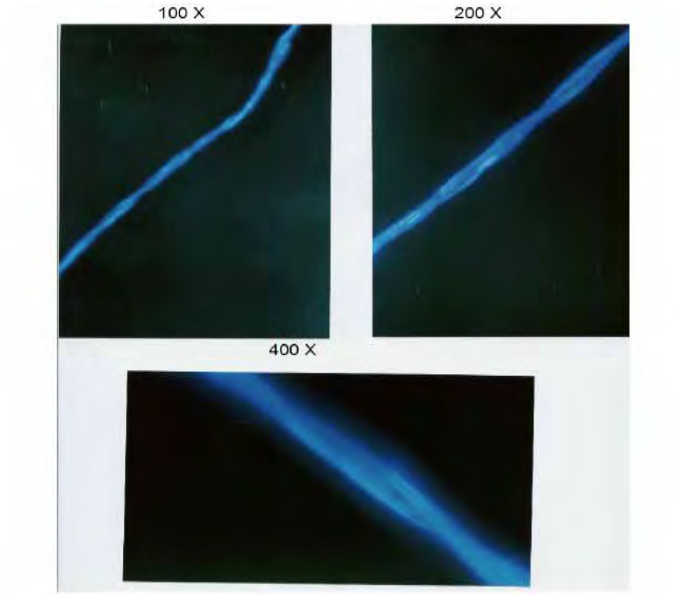

Figure 5- Fluorescence micrography image of a DNA aggregate whose ψ-spectrum is shown in reference 13. The PEG concentration is 150mg/ml and the NaCl concentrations is 0.2M.The magnification is shown on the top of each picture. The DNA was stained with DAPI.

A question which arises quite naturally from what was said may be formulated in the following terms: what are the flexible polymer critical concentrations needed to induce phase separation (*i.e.*, to induce the DNA condensation) as a function of the salt concentration? Since we know that the DNA molecules have a high charge density (one elementary charge each 1.7Å) we should expect the critical PEG's concentrations (PEG_{crit}) to strongly depend on the salt concentration. If so, can we measure this quantity (PEG_{crit} as a function of the NaCl concentration)?

In the paper 1[13], we present a suitable experimental strategy which enabled us to answer this question *i.e.*, we present the whole phase diagram for the **ψ**-condensation experimentally determined using circular dichroism spectroscopy, including the phase boundaries for the condensation transition as well as for the reentrant decondensation transition.

In our experiments, we chose the dispersion's optical activity as the order parameter to locate the onset of the DNA condensation: once the dispersion exhibits an anomalous optical activity or **ψ**-spectrum (in comparison with the DNA dispersion optical activity), we assign to those physicochemical conditions the presence of condensed DNA. Upon increasing the PEG's concentration beyond the PEG_{crit}, we observed the loss of **ψ**-spectrum and likewise we assign to those physicochemical conditions the dissolution of the condensed DNA. It is worthwhile to mention at this point that the reentrant decondensation transition had already been observed for DNA mono molecular condensation [14] and also predicted on pure theoretical grounds by Grosberg *et al* [15] and de Vries[16].

In this way, we were able to measure the PEG_{crit} concentrations for both condensation and reentrant decondensation transitions as a function of the medium ionic strength. The experimental results are presented in perspective along with previously obtained experimental data for similar systems and are also compared with the prediction of a theoretical model which estimates the location of the phase boundary for the **ψ**-condensation. The model is in quantitative agreement with the experimental data concerning the condensation transition; as far as the reentrant decondensation is concerned, the model does not predict the entire phase boundary due to its premise [16]. This theoretical problem is readdressed in the manuscript included in this thesis [17].

Paper 2

Summary

It is known from cytology that the genome of the prokaryotic organism (*Archaea* and *Bacteria*) is not enclosed within a membrane such as the one which may be found in the eukaryotic cells (the nuclear membrane which segregates the cells DNA from the cytoplasm) and it is in direct contact with the cytosol [18]. The lack of a confining membrane however, does not prevent the bacterial chromosome to fill only a fraction (≈ 25%) of the entire cell's volume [19]. A question which arises quite naturally from this experimental finding may be formulated as follow: what interactions do not allow the DNA segments to get as far as possible from each other and thus occupy the entire cytosol? In other words, why is the bacterial cytosol *a poor solvent* for the DNA molecule?

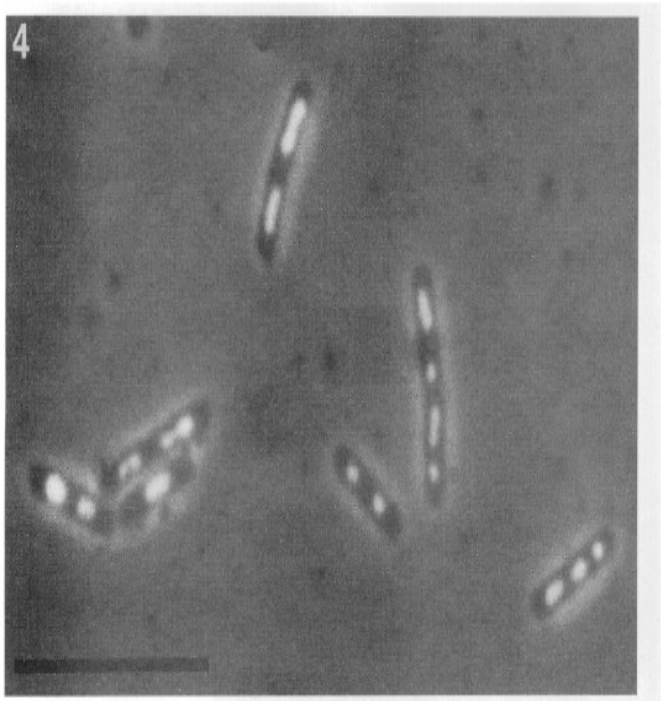

Figure 6 – The bacterial nucleoid (bright spots) of the bacteria *B. subtilis* obtained by means of fluorescence and phase contrast microscopy (bar = 8 μm). Robinow,C and Kellenberg,E. *Microbiologiacal Reviews*.**1994** (58):211-232.

The seminal experiments performed by Murphy and Zimmerman [20] have given us some clues to answer this question and so enlighten the formation and stability of the nucleoid structure. These authors carefully analyzed the effects of the cell's cytosol components on DNA fragments extracted from phages. The cytosol components were separated according to its affinity for the DNA in to two different fractions: the DNA-binding fraction (mainly composed of cationic proteins) and the DNA-non binding fraction. Experiments performed *in vitro* made clear that neither the DNA-binding fraction nor the DNA-non binding fraction were able to condense the DNA alone, even at much higher nominal concentrations than the ones inside the cell. However, the two cytosol fractions were able to readily precipitate the condensed DNA by means of centrifugation. The synergism between crowding and electrostatic interactions on the bacterial nucleoid *in vivo* was stated for the first time.

In the paper 2[21], we discuss the results obtained by those authors as well as the underlying physical mechanism responsible for such synergism along the lines of the de Vries' theory for polymer-induced DNA condensation [16]. Additionally, we performed light scattering and agarose gel electrophoresis experiments (a similar assay performed by Murphy and Zimmerman) in order to generalize their conclusions.

In our experiments, we used the positively charged protein sso7d (which mimics the cytosol protein DNA-binding fraction) extracted from the Archaebacteria *Sulfolobus solfataricus* and the neutral polymer PEG (which mimics the DNA-non binding fraction). At physiological conditions *i.e.*, pH=7.0 and [NaCl] =0.15M, we found that none of these components separately were able to condense the plasmid pUC18 alone but here again, together the protein sso7d and the PEG efficiently were able to do it.

Resting upon assumptions concerning the phase separation in a mixture of semi-flexible poly-electrolyte and neutral polymers [16], we were able to build a sharp picture for the mechanism behind the observed synergism and state in a very general way that the DNA molecules complexed with cationic proteins (the sso7d protein in our experiments) are much more susceptible to **ψ**-condensation than the naked DNA molecule due to *its lower charge density and higher effective diameter* (see figure 7). These are the molecular bases of our experimental findings and as our experiments suggest [21], this is a very general mechanism for DNA compaction inside prokaryotic cells [19, 20].

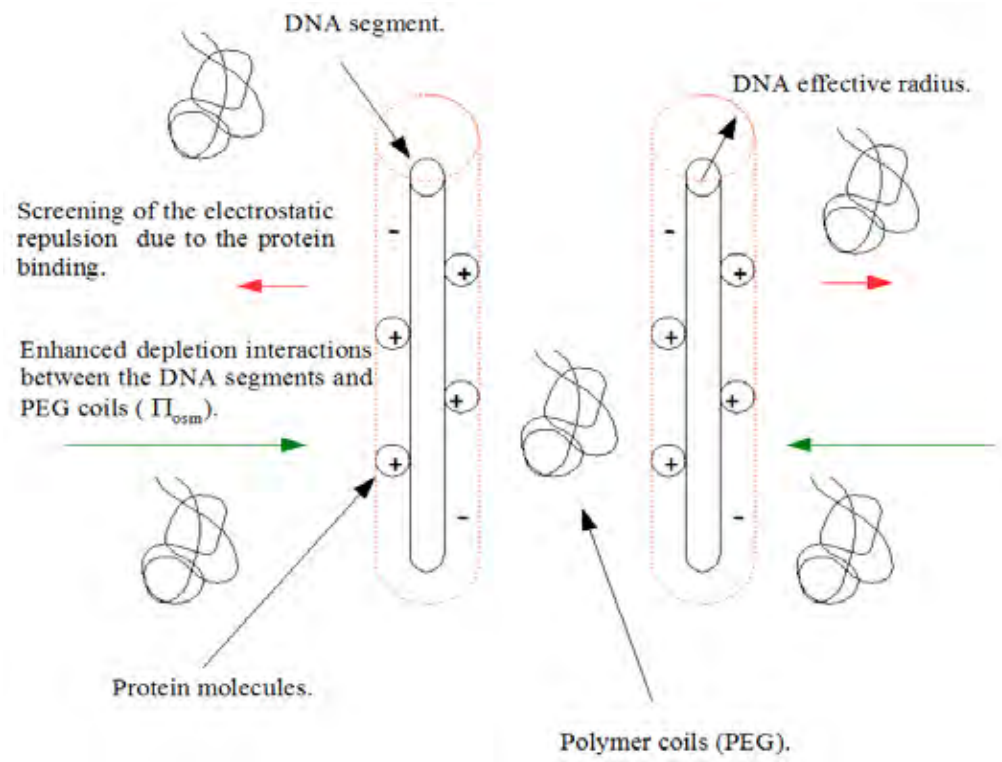

Figure 7 – Representation of the DNA/PEG/protein colloid mixture and the most important interactions among them. The screening of the electrostatic repulsion among the DNA segments due to the positively charged proteins bound and the enhancement of the depletion interactions due to the thicker DNA/protein complexes efficiently cooperate to promote the DNA condensation.

Paper 3

Summary

In the middle of 60s, Vinograd and co-workers [22] opened a totally new chapter in the study of the DNA conformation. These authors inferred from sedimentation measurements that the DNA extracted from the polyomavirus could exist in two different conformations: one much more compact than the other. Electron micrographies made clear that the compact form was a circularly closed DNA molecule whose axis was coiled upon itself (the super-coiled DNA) and the less compact conformation was a circularly opened DNA molecule without super-coiling (see figure 8). They also discovered that the compact form could turn in to the less compact one once a single break was introduced along one of the DNA strands by specific enzymes: the single break released the twist stored in the DNA molecule reducing the level of super-coiling to zero (nicked DNA).

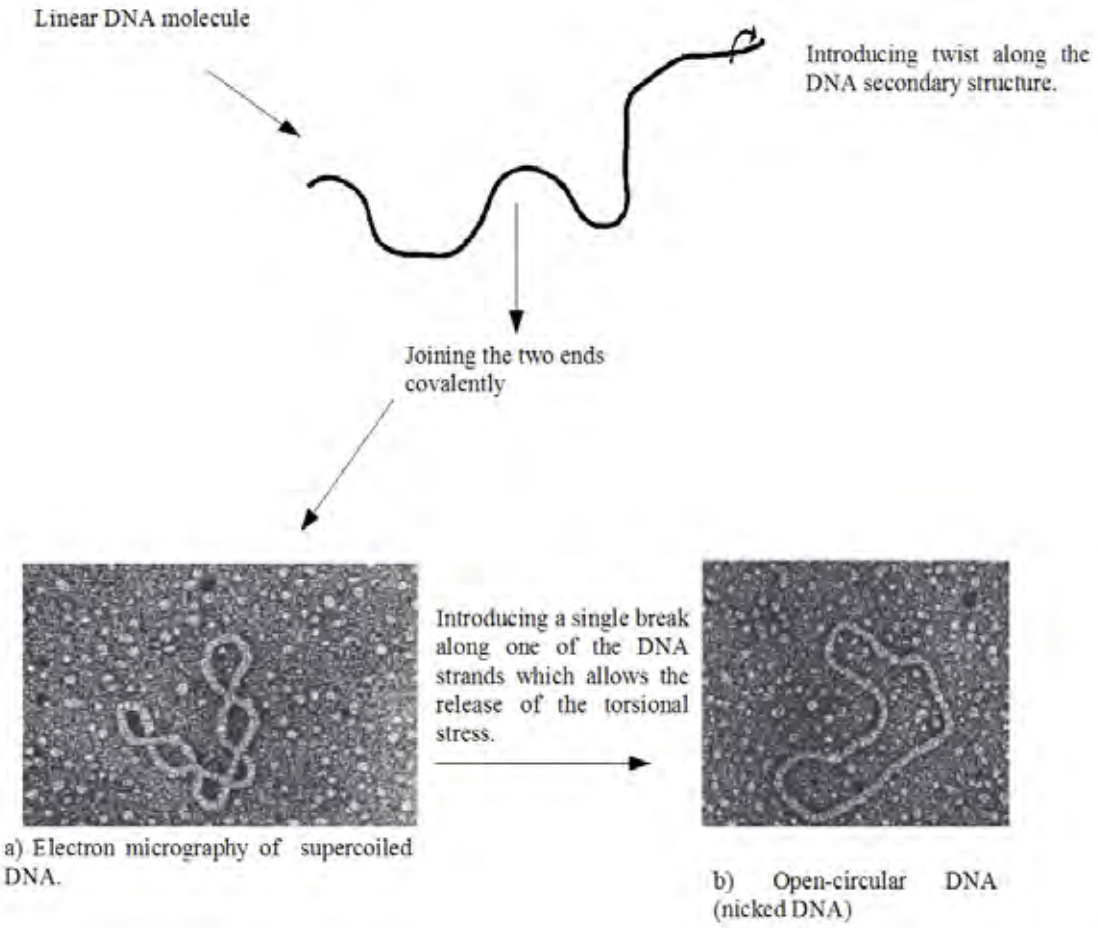

Figure 8- Illustration of a linear DNA molecule, the super-coiled form obtained from the linear one by twisting one DNA's end keeping the other fixed (a). A single break in one of the DNA strands releases the twist and allow the conversion of the super-coiled (circularly closed) form in to the circularly open form (nicked DNA).

Such compact DNA conformation or super-coiled DNA turned out to be very common in nature: we find super-coiling in the bacterial and viral genome as well as in the mitochondrial and chloroplast DNA [23]. Over the years, intense experimental research has shown that super-coiling is of fundamental importance for some biological functions: a little decrease in the level of super-coiling may forbid the correct duplication and partitioning of the bacterial genome among the daughter cells [24].

In the DNA **ψ**-condensation context, only a few studies have focused on the influence of the DNA topology on the phase separation and to some extend, it has been implicitly assumed that the super-coiled DNA conformation does not influence the process at all *i.e*., linear and super-coiled DNA have the same behavior in a crowded environment.

In the paper 3 [25], we experimentally compare the **ψ**-condensation of both linear and super-coiled forms of the plasmid pUC18 by means of agarose gel electrophoresis. We analyze the DNA content in the supernatant of PEG/pUC18 and PEG/linearized pUC18 dispersions and estimate the critical PEG concentrations (PEG_{crit}) needed to induce the condensation of both forms. The experimental results suggest that super-coiling indeed exert almost no influence on the PEG thresholds, although a slightly higher PEG_{crit} concentration is needed to induce the condensation of the super-coiled pUC18.

Numerical estimates were performed in order to explain this experimental finding. To do that, the free energy of super-coiled DNA dispersed (free) in solution and inside the condensates was estimated along the lines of de Vries theory for polymer-induced DNA condensation [16]. In this theory, the location of phase boundary for the DNA condensation is estimated calculating both the insertion free energy of a linear DNA molecule ($f_{ins,free}$) per unit of length in a solution containing the flexible polymer and the insertion free energy of the condensed DNA ($f_{ins,cond}$) again per unit of length in the same solution. To estimate the PEG_{crit} concentrations as a function of the monovalent salt concentration, the following equality is imposed: $f_{ins,free} = f_{ins,cond}$.

The insertion free energy of the linear DNA in a polymer solution is calculated multiplying the solution osmotic pressure times the volume of a DNA segment immersed in the solution [16]. In order to compare the insertion free energy of both linear and super-coiled DNA, we must take into account that the correlation length of the polymers solution is usually smaller than the diameter of the plectonemic conformation [26] which is the case of our experimental system, and so $f_{ins,free}$ should be linear with respect to the contour length of both linear and super-coiled DNA (see figure 9) *i.e*, the chemical potential of these two conformations should be roughly the same at identical solution conditions.

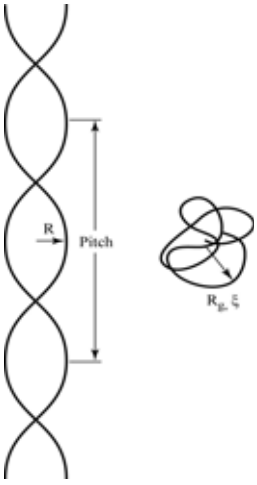

Figure 9 – Illustration of the ideal plectonemic conformation (the double helix) and a polymer coil ("coil-like" continuous curve) along with the length scales relevant to estimate $f_{ins,free}$ of the super-coiled DNA. Since the radius *R* of the plectonemic conformation is typically larger than the solution correlation length (R_g ,ξ), we should not expect any difference in the insertion work of the free super-coiled DNA relatively to the free linearized form.

On the other hand, the insertion free energy of the condensed super-coiled DNA $f_{ins,cond}$ may be estimated in a first approximation, assuming that the strength of the interaction among the DNA super-coils inside the condensate is nearly equal to the one among the linear DNA molecules or, in other words, that the super-coil may be approximated by to parallel DNA linear molecules whose distance equals the plectonemic diameter. If this is the case, our numerical estimates show that the free energy associated with the mechanical conformational changes necessary to pack the DNA super-coils inside the condensate is only a small fraction of the total packing free energy which is dominate by the electrostatic repulsion among the DNA segments and by the tight confinement of a semi-flexible polymer inside a tiny volume.

Here again we consider that the insertion osmotic work is the same for both super-coiled and linear DNA, and we also neglect any amount of flexible polymer which may remains inside the condensed phase. If there were big difference in the packing free energies of both DNA conformations, we would had certainly seen a shift in the experimentally determined phase boundary for the pUC18 plasmid in comparison with its linearized form. Since this is not the case, we should not expect any significant super-helical unwinding but only a small perturbation in the super-helix radius, which may be the source of the slightly higher PEG_{crit} concentrations for the super-coiled DNA.

In order to portrait a sharper physical picture of the conformation of the super-coiled DNA inside the condensate, Monte Carlo simulations were performed. Actually, one might ask how the super-coiled DNA does look like inside the condensed phase (in comparison with the ideal plectonemic conformation). Is it possible that upon confinement the DNA unwinds significantly or further more, in order to fit the DNA inside the tiny condensate volume the plectonemic diameter decreases? Our numerical estimates have already given us some clues. To answer these questions with more accuracy, the super-coiled DNA was modeled at a coarse grained level as a circularly closed string with beads (the "bead-string" model for polymers) and the effects of the environment on the DNA molecule were modeled by a nematic field which tends to align the plectonemic axis along the nematic director **n**. The topological restrictions are imposed by the relation [26]:

$$Lk = Wr + Tw \qquad (1)$$

In the equation (1), Lk represents the DNA link number which measures the number of helical turns in a circular DNA molecule, Wr represents the writhe which measures the number of cross-overs of the DNA super-coiled axis upon itself and Tw represents the twist which measures the excess (or deficit) of helical turns relative to the relaxed conformation (see figure10). The Hamiltonian of the system is written as:

$$H[\mathbf{r}_1, \mathbf{r}_2, \mathbf{r}_3, \ldots \mathbf{r}_N] = \tfrac{1}{2} k_s \Sigma(\left| (\mathbf{r}_{n+1} - \mathbf{r}_n) \right| - l_b)^2 + \tfrac{1}{2} k_b \Sigma (\arccos(\left| (\mathbf{t}_{n+1} - \mathbf{t}_n) \right|))^2 + 2\pi^2 k_t (\Delta Lk - Wr)^2/N + \Sigma U_{ele}(\left| (\mathbf{r}_{n+1} - \mathbf{r}_n) \right|) + \Delta N [\mathbf{r}_1, \mathbf{r}_2, \mathbf{r}_3, \ldots \mathbf{r}_N] \qquad (2)$$

The first term in the Hamilton's function $H[\mathbf{r}_1, \mathbf{r}_2, \mathbf{r}_3, \ldots \mathbf{r}_N]$ accounts for the stretching energy between two consecutive monomers (represented by spheres in the "bead-spring" model) located by the vectors $\mathbf{r}_n$; the second term accounts for the bending energy, since the DNA is an intrinsic semi-flexible molecule and the vectors $\mathbf{t}_n$ are vectors connecting the center of two consecutive spheres; the third term represents the twisting energy and is written as a function of the linking number and the writhe; the fourth term accounts for the electrostatic interaction between the spheres in the Debye-Hückel approximation.

The last term represents the interaction between the DNA segments and the nematic field as well as the interaction induced between two DNA segments which belong to the same molecule by the depletion of a segment which belongs to the surrounding molecules. The meaning of each constant in the Hamiltonian and the details of the simulation may be found in reference 25.

The results of the Monte Carlo simulations showed that we should not expect for a strong unwind (conversion of the writhe in twist) of the DNA molecule in typical cases but rather a decrease in the plectonemic diameter [25] in agreement with earlier experimental findings [27].

Figure 10 – Illustration of DNA conformations using a "tube model". The open circular DNA without any twist (relaxed conformation) is represented in (a). The circularly closed DNA with twist (Lk=-4 and Tw = -4) is shown in figure (b). Conversion of part of the twist in writhe (Wr ≈ -4 and Tw ≈ 0) (c) and (Wr ≈ -3 and Tw ≈ -1) (d).The angle γ represents the super helix winding angle.

Manuscript

Summary

The experimental results presented in paper 1 [13] may be understood once we consider the depletion interactions between the poly-electrolyte segments (DNA segments) and the flexible polymer (PEG): the flexible polymer's configuration entropy decreases upon confinement among the DNA segments; therefore the local polymer's concentration should be lower among the poly-electrolyte segments than in the bulk of the solution. The difference in the polymer's local concentration induces an effective attractive interaction among the DNA segments due to the unbalanced osmotic pressure [5] (see the introduction) which ultimately leads to the DNA condensation.

The observed dependence of the PEG_{crit} upon its degree of polymerization (N) is thus a natural consequence of the polymer confinement: relatively large polymer coils have their configuration space much more reduced than the small ones or in other words, larger polymer coils have many more degrees of freedom "frozen out" in order to fit among the DNA segments than the smaller ones, which in turn, can move in to and out from the DNA molecule without a high entropy cost.

The statistics of confined flexible polymer chains may be described by the *Edwards equation*, a diffusion-like equation which governs the probability distribution function $G(\boldsymbol{r}, \boldsymbol{r_o}, \boldsymbol{N})$ for the end-to-end distance of a polymer chain [28]:

$$- l_k^2/6\, \nabla_r^2\, G(\boldsymbol{r},\boldsymbol{r_o},N) + V(\boldsymbol{r}) G(\boldsymbol{r},\boldsymbol{r_o},N) / K_B T = - \partial_N\, G(\boldsymbol{r},\boldsymbol{r_o},N) \qquad (3)$$

In the equation 3 the symbol ∇^2 represents the conventional Laplace operator which acts on the chain endpoint coordinate $\boldsymbol{r}$ whereas $\boldsymbol{r_o}$ locates the other chain endpoint. The chain is composed of N monomers and the distance between two consecutive monomers is represented by l_k (Kuhn segment). The symbol ∂_N represents the partial derivative of $G(\boldsymbol{r}, \boldsymbol{r_o}, N)$ with respect to N; $V(\boldsymbol{r})$ represents the potential energy of a monomer at the position $\boldsymbol{r}$. The Boltzmann constant is represented by K_B and T represents the absolute temperature. Once we know the probability distribution function $G(\boldsymbol{r},\boldsymbol{r_o},N)$ for a chain under certain physical conditions, the thermodynamics of the system may be determined *i.e.*, we may calculate the thermodynamics quantities of interest such as the chemical potential or the osmotic pressure of the polymer chain in such a way that we can fully describe the interactions between the chain and the confining DNA segments. In the manuscript [17] we solved the Edwards equation analytically assuming that the polymer chain is confined within "a cylindrical cell" and evaluated $G(\boldsymbol{r}, \boldsymbol{r_o}, N)$ explicitly.

The second interaction which must be considered in describing the phase behavior of neutral polymer mixtures is concerned with the interaction among these macromolecules which may be relevant even at small concentrations (volume fraction around 1%) for polymers of high molecular weight [29]. Therefore we must include in our description the interactions among the flexible polymer chains and also take into account possible deviations from the scaling predictions when the scaling regime ($N \rightarrow \infty$) is not attained. These interactions have been shown to be important and to modify even qualitatively the phase behavior of flexible/semi-flexible polymer mixtures [30].

In our model, the deviations from the scaling regime are explicitly considered by empirical corrections in the scaling exponents in order to generalize our conclusions about the phase behavior of such mixtures whatever the relevant length scales which characterize the neutral polymer solution.

The third relevant interaction is the interaction among the DNA segments. This interaction is accounted by a truncated expansion of the osmotic pressure of rigid cylinders in terms of its numerical segment density [30] and DNA poly-electrolyte nature is introduced along the lines of Odijk's theory for excluded volume in poly-electrolyte solutions [31]. We assume that each DNA segment is a rigid cylinder within the scale of its persistence length (50 *nm*). The electrostatic repulsion among them is accounted by an effective radius which depends on the salt concentration and in a first approximation may be written as the DNA bare radius (≈1,2 *nm*) plus the electrostatic relevant length scale: the Debye length κ^{-1} which is a function of the medium ionic strength.

In order to draw some general conclusion about the phase behavior of such dispersion, we impose the equality of the osmotic pressure and chemical potential of the polymer coils inside the volume occupied by the DNA molecule and in the bulk of the solution. The numerical analysis is carried out for some typical values the PEG's degree of polymerization (*N*) and the values of all other parameters are taken from known experimental measurements.

The results show that above a flexible polymer critical concentration (PEG_{crit}), the segment density inside the DNA molecule "jumps" from its characteristic value obtained at disperse solution to a higher one, thus defining the onset of the DNA condensation: the depletion interactions overcome the repulsion interaction among the DNA segments. Here we notice that the small PEGs coils are less efficient to induce the DNA condensation than the large ones, since these molecules are hardly partitioned between the two phases or in other words, they can enter the condensed phase without any high hindrance in contrast with what happens with the PEGs coils of higher molecular weight. This conclusion has been confirmed by experiments with PEGs of different molecular weights [13].

A peculiarity of neutral polymer solutions must be pointed out here in order to highlight some results obtained from the numerical calculations. The structure of the neutral polymer solution strongly depends on its concentration: in the dilute regime, when the molecules are far from each other and hardly interact, the relevant length scale for the solution's thermodynamics is the radius of gyration of the polymer coils which scales with the number of monomers as $R_g \sim N^{3/5}$. For higher concentrations, the coils start to overlap and the characteristic solution length scale is the correlation length ξ which scales with the polymer volume fraction ϕ as $\xi \sim \phi^{-3/4}$ and is independent on *N* once the scaling regime is reached [32]. Therefore, the cross-over from the dilute to semi dilute regime involves a change in the strength of the interactions between the flexible polymer and the DNA segments in a way that the intensity of the depletion potential starts do decrease above a certain PEG's concentration know as overlap concentration (ϕ^*) and leads to the dissolution of the condensed phase. The dissolution of the condensed DNA is also found in our theory: above a certain PEG_{crit} concentration, the segment density inside the condensate "jumps" back to its dispersed value which defines the onset of the DNA reentrant decondensation. This fact is also in agreement with the experiments. A more detailed discussion may be found in the accompanied manuscript bellow.

Introdução

Entre os diversos tipos de misturas que encontramos naturalmente ou que produzimos existem dois grandes grupos: as misturas homogêneas (soluções) e as misturas heterogêneas (dispersões e suspensões). A diferença física essencial entre esses tipos de misturas reside no tamanho das partículas dissolvidas. No caso das soluções, as partículas possuem dimensões da ordem de Angstroms ($1\ \mathring{A} = 10^{-10}\ m$) enquanto que nas misturas heterogêneas (dispersões) as partículas dispersas tem usualmente dimensões características da ordem de alguns nanômetros ($1\ nm = 10^{-9}\ m$) até alguns micrometros ($1\mu m = 10^{-6}\ m$). Misturas cujas partículas possuem dimensões características variando nesse intervalo são definidas como dispersões coloidais e as partículas dispersas denominadas colóides [1].

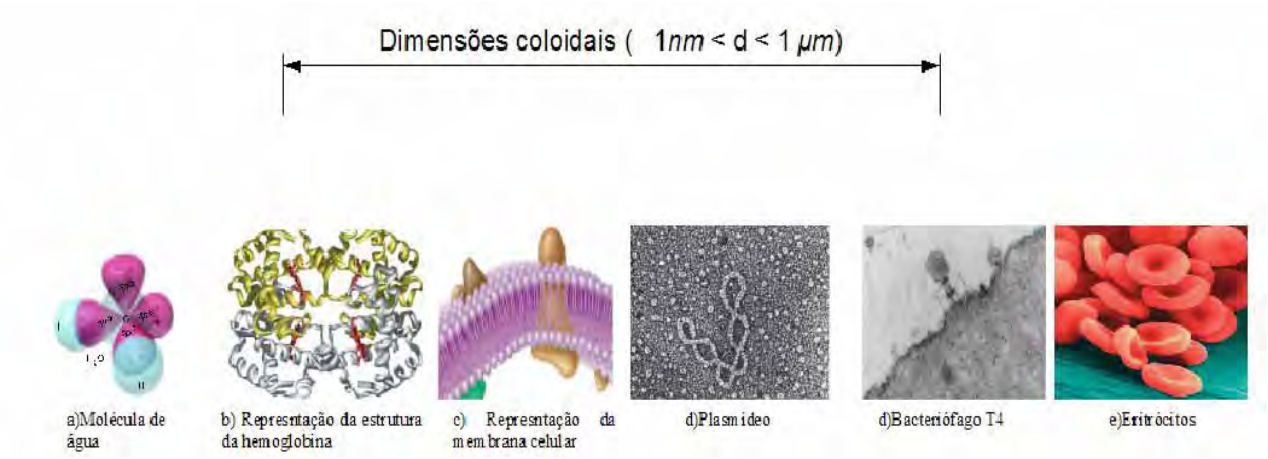

Figura 1 - Dimensões características dos sistemas coloidais($1nm < d < 1\ \mu m$). Localização da "região coloidal" em sistemas de interesse físico e biológico: a) representação dos orbitais moleculares da molécula de água; b) representação da estrutura quaternária da molécula de hemoglobina; c) representação da membrana plasmática de uma célula eucariótica; d) eletromicrogafria do plasmídeo pUC 18; e) eletromicrografia do fago T4 ligado a parede celular bacteriana. f) eletromicrografia de hemácias (eritrócitos). Ilustrações retiradas do livro "Biologia Celular e Molecular" Lodish,H *et al* .5ª Edição -Editora Artmed.

O comportamento físico das dispersões coloidais é um reflexo direto dessa característica mais elementar. Devido as suas dimensões, as partículas coloidais interagem fortemente entre si bem como com campos externos. Dessa forma, é possível, e.g., separar seus componentes mediante campos de força externos (a ação da gravidade, ultra-centrifugação) ou determinar as dimensões das partículas dispersas mediante espalhamento de luz, o que não é estritamente possível para as soluções (tomemos como exemplo mais simples uma solução de cloreto de sódio) [1].

Uma vez feitas essas considerações iniciais, delimitaremos o escopo da presente tese: - o estudo de dispersões coloidais constituídas de polímeros neutros e polímeros eletricamente carregados (polieletrólitos). O comportamento de fase de dispersões coloidais assim constituídas é atualmente um dos mais proeminentes campos de pesquisa teórica e experimental em físico-química com desdobramentos técnicos e científicos muito amplos: o entendimento dos mecanismos envolvidos na complexação/condensação entre macromoléculas biológicas nas células vivas e a conseqüente regulação dos processos fisiológicos celulares [2 e ref.citadas], o desenvolvimento de tecnologias para purificação e reutilização de águas, o melhoramento da qualidade dos produtos da indústria alimentícia e o desenvolvimento de mecanismo de "entrega" de fármacos a órgãos específicos para o

tratamento de doenças constituem algumas aplicações do conhecimento adquirido a partir do estudo dos colóides.

Um marco para o desenvolvimento e síntese teórica desse campo de interseção, por excelência, entre a física e a química, é sem dúvida a teoria **DLVO** [3], desenvolvida independente por **D**eryaguin e **L**andau na Rússia e **W**erwey e **O**verbeek na Holanda. De acordo com as premissas dessa teoria, a estabilidade das dispersões coloidais é determinada pelo balanço entre as interações eletrostáticas (descritas pela equação de Poisson-Boltzmann) e as interações de van der Walls: o comportamento de fase das dispersões coloidais resulta da competição entre as interações eletrostáticas repulsivas de longo alcance (que numa primeira aproximação podem ser calculadas pelo modelo de Debye-Huckel para soluções eletrolíticas) e as interações atrativas de curto alcance de van der Walls. Não obstante as inúmeras restrições impostas à validade da teoria DLVO por experimentos precisos e teorias mais refinadas, seus fundamentos ainda são invocados como base para a interpretação do comportamento de fase dos colóides desde a sua publicação *in totum* [4].

Paralelamente a esse desenvolvimento teórico no qual funções contínuas descrevem interações *à distância* entre partículas carregadas, Asakura e Oosawa hipotetizaram *que restrições espaciais locais* impostas por determinadas macromoléculas dispersas às demais, em virtude de seu volume finito, poderiam influenciar significativamente o comportamento de fase dessas misturas, em particular, daquelas misturas de importância biológica [5]. Na sua célebre nota **"On interactions between two bodies immersed in a solution of macromolecules"**, esses autores explicitamente indicaram que uma vez que solutos não possuam acesso a determinadas regiões da solução, um *potencial atrativo local* é estabelecido.

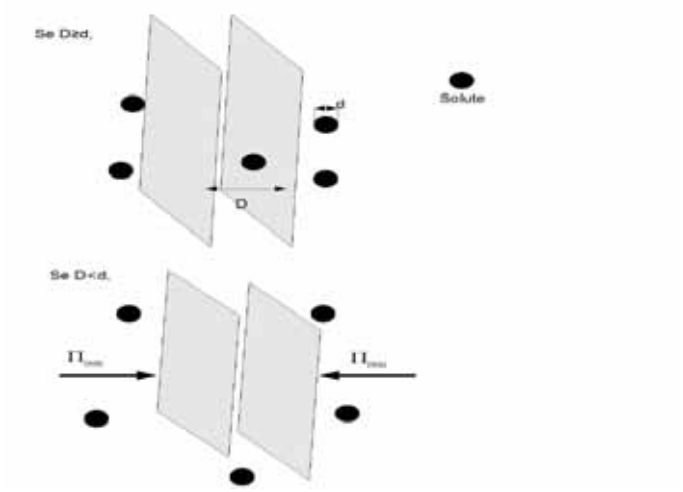

Figura 2 - Ilustração da depleção do soluto (esferas) da região entre as superfícies planas quando da existência de impedimentos espaciais (*i.e.*, quando a separação entre as placas é menor que o diâmetro das moléculas do soluto, $D < d$) e da conseqüente pressão osmótica exercida pelo soluto sobre a superfície externa das placas.

O potencial atrativo inicialmente proposto é conhecido atualmente como potencial de depleção e as interações dele decorrentes como **interações de depleção**. A literatura científica sobre esse tópico tem crescido enormemente desde então e as interações de depleção tem sido invocadas para explicar uma variedade de fenômenos tanto *in vitro* como *in vivo*: fenômenos diversos e aparentemente não relacionados, como a formação de cristais de proteínas em solução [6] e a formação e manutenção da estrutura do nucleóide em organismos procariotos, tem sido entendidas ao longo dessa mesma linha teórica [7].

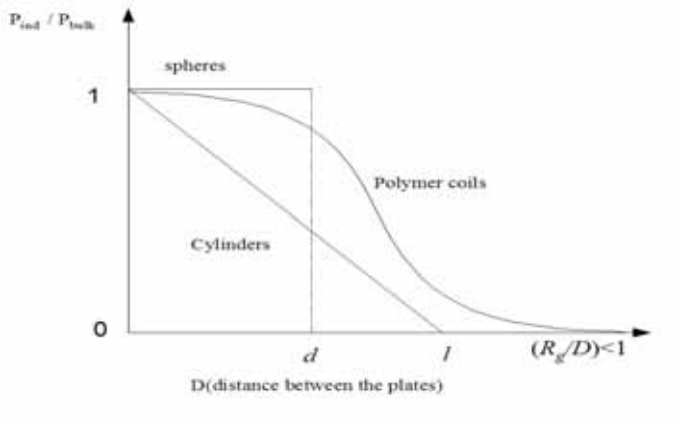

Figure 3 – Ilustração das interações de depleção expressa em termos da pressão osmótica induzida (normalizada pela pressão osmótica da solução P_{bulk} para o caso de esferas rígidas de diâmetro *d*, cilindros de comprimento *l* e moléculas poliméricas de raio de giro R_g em função da distancia *D* entre as placas..

No caso do soluto ser modelado como esferas rígidas, o potencial de depleção varia descontinuamente [5]; potenciais um pouco mais complexos aparecem quando o soluto é um polímero: nesse último caso, as dimensões do polímero distribuem-se em torno de um valor médio (raio de giro do polímero - R_g) sendo que o potencial varia continuamente em função da distância entre as placas. O particionamento do polímero entre a solução e o espaço entre as superfícies interagentes impede as descontinuidades nas interações.

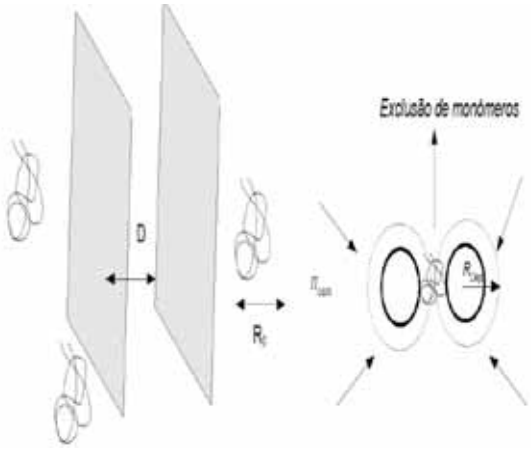

Figura 4 - Depleção das moléculas do polímero da região entre as superfícies planas quando $D < R_g$ e da região entre as duas superfícies esféricas. As moléculas do polímero são apresentadas por curvas continuas (conformação "coil-like") e os círculos hachurados em volta das esferas representam as camadas de depleção ("depletion layers").

O conteúdo substancial dessa tese trata das interações depleção que ocorrem em sistemas biológicos cujas implicações são tão significativas quanto às implicações de interações outras (eletrostáticas, forças de dispersão *et cetera*) em diferentes situações experimentais-modelos, bem como dos elementos teóricos desenvolvidos (analíticos e computacionais) para um melhor entendimento das implicações das interações de depleção. O que segue é um resumo sucinto de cada artigo da tese (no total de quatro) nos quais as idéias e resultados centrais estão sumarizados.

A partir da leitura desses sumários, deve ficar clara a intersecção e a coesão entre o conteúdo dos artigos, substância última dessa tese.

Artigo 1

Sumário

Com a descoberta da condensação-**psi** (condensação **i**nduzida por **p**olímero e **s**al ou condensação- **ψ**) por Lerman do ácido desoxirribonucléico (DNA) [8] o estudo do DNA no estado líquido-cristalino inicia-se: por um lado os condensados de DNA têm sua estrutura como alvo de estudo em virtude da possibilidade de medirem-se as interações inter-moleculares responsáveis pela morfologia, dimensões e estabilidade. Em particular, a possibilidade de medir-se com acuràcia forças entre segmentos de DNA em função de suas distâncias via difração de raios-X [9], promove desdobramentos experimentais que forçam a teoria a desenvolver-se no sentido de sistematizá-los [10,11] com o desenvolvimento do formalismo mecânico-estatístico para polieletrólitos semi-flexíveis no estado de agregação líquido-cristalino.

As interações responsáveis pela da separação de fase na mistura polímero flexível/poli-eletrólito semi-flexível, por outro lado, constituem um assunto de investigação paralelo: nessa vertente são inquiridas as causas da transição solução isotrópico/cristal líquido.

Em 1972, Jordan *et al* [12] realizaram experimentos de espectroscopia de dicroísmo circular (EDC) em soluções concentradas de DNA extraídos dos fagos T4 e T7 e constatou-se pela primeira vez a atividade ótica anômala apresentadas por agregados de DNA formados em certas condições físico-químicas da solução (acima de certas concentrações críticas de poli (etilenoglicol) (PEG) e cloreto de sódio (NaCl)). Não obstante as limitações técnicas, foi sugerido que a estrutura terciária ou supramolecular dos agregados fosse responsável pela absorção seletiva de um dos estados de polarização da luz circularmente polarizada incidente sobre a amostra (dicroísmo circular).

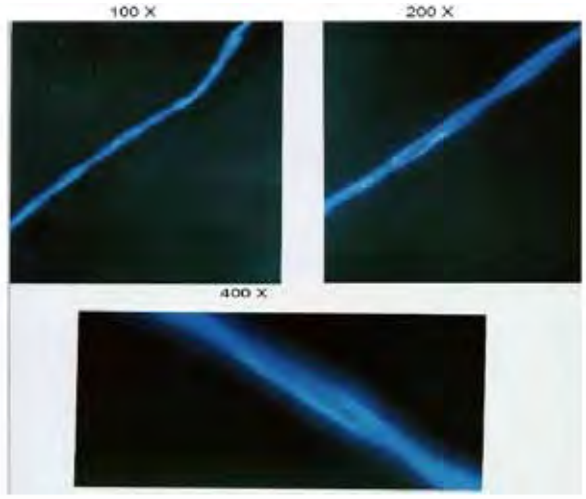

Figura 5 - Fotografia obtida por microscopia de fluorescência de agregados de DNA linear (extraído de timo de bezerro). A concentração do DNA é estimada em 40 μM (em pares de base) e as concentrações do PEG e [NaCl] são respectivamente 150 mg/ml e 0.2 M. As ampliações estão dadas na parte superior de cada fotografia. O marcador fluorescente usado foi o DAPI.

Uma questão que se naturalmente coloca é, pois: quais as concentrações críticas do polímero flexível e do sal monovalente necessárias para induzir a formação de tais agregados? Uma vez que o DNA é um polímero carregado (uma carga elementar a cada 1.7 Å) deve-se esperar que a repulsão entre seus segmentos dependa fortemente da força iônica da solução e da quantidade de polímero depletado (número de moléculas com seu espaço configuracional reduzido devido ao confinamento pelos segmentos do polieletrólito) *i.e*., das forças de depleção que tendem a aproximar os segmentos.

No artigo 1 desta tese, as concentrações críticas do polímero neutro PEG necessárias para induzir a transição-ψ em função da concentração molar do NaCl (cloreto de sódio) são estimadas utilizando-se a espectroscopia de dicroísmo circular. O parâmetro de ordem escolhido para localizar a transição é a atividade ótica da solução: variam-se as condições físico-químicas da solução (concentração de PEG (% em massa) e de [NaCl]) e quando do aparecimento de espectros de absorção do tipo-ψ (espectro-ψ) têm-se a concentração crítica do polímero flexível (PEG_{crit}) em função da concentração molar do sal monovalente NaCl. Faz-se necessário também notar que (e este é um ponto que será alvo de um estudo mais detalhado no capítulo 4) para concentrações acima do PEG_{crit}, o espectro-ψ desaparece e a solução volta a ser oticamente isotrópica, em outras palavras, os agregados de DNA ressolubilizam. As concentrações críticas para a transição reversa (descondensação) também foram estimadas e o diagrama de fase completo da transição construído [13]. A ressolubilização dos condensados de DNA é um fenômeno que foi inicialmente observado em transições monomoleculares de DNA [14] e previsto por Grosberg *et al* [15] e de Vries [16] e está intimamente relacionado com os comprimentos de escala relevantes para descrever o comportamento de soluções semi diluídas de polímero neutro em função de sua concentração.

Os resultados experimentais obtidos são comparados com as previsões teóricas do modelo proposto por de Vries [16] para descrever a condensação de polieletrólitos semi flexíveis induzidas por polímero neutro e acordos parciais são verificadas: não obstante o sucesso da descrição quantitativa da condensação-ψ, o modelo descreve apenas qualitativamente a transição reversa. Os achados empíricos, no entanto, são suficientes para motivar um estudo teórico mais detalhado do comportamento de fase dessas misturas e uma descrição mais detalhadas das interações existentes, especialmente entre o polímero flexível e a molécula de DNA. Tal estudo é desenvolvido no manuscrito da presente tese [17].

Artigo 2

Sumário

Sabe-se a partir de estudos citológicos, que o nucleóide dos organismos procariotos (*Archaea* e *Bacteria*) não é envolvido por membrana nuclear (a carioteca, presente nos organismos eucariotos e que separa o genoma do citoplasma celular) estando o cromossomo em contato direto com o protoplasma [18]; não obstante a ausência de membrana, o nucleóide bacteriano e.g., ocupa apenas uma fração do volume celular total (≈ 25%), portanto não o preenchendo totalmente [19]. A pergunta que se coloca naturalmente é, pois: que forças confinam o genoma bacteriano, impedindo que os segmentos de DNA se afastem o máximo possível? Em outras palavras, por que o protoplasma procarioto não é um bom solvente para o DNA?

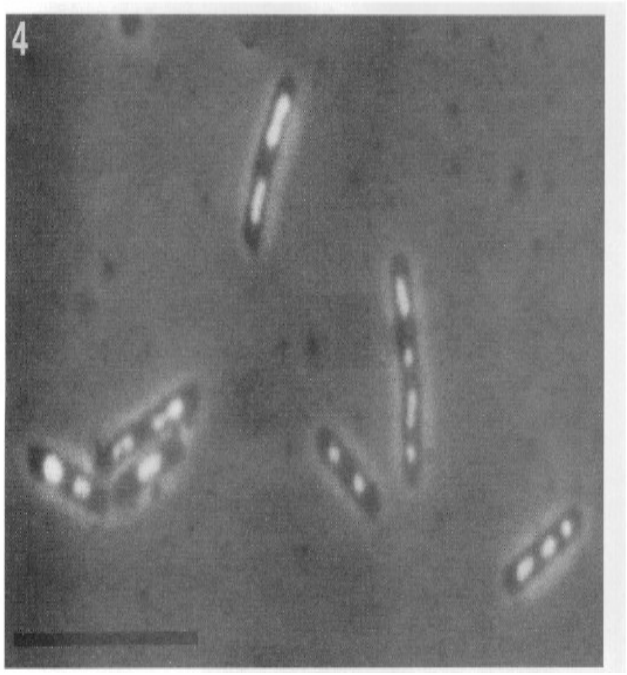

Figura 6 – Fotografia da bacteira *B. Subtilis* obtida pela combinação de microscopia com contraste de fase e microscopia de fluorescência (barra = 8 μm). Robinow,C e Kellenberg,E. *Microbiologiacal Reviews*.**1994** (58):211-232.

Os experimentos seminais realizados por Murphy e Zimmerman [20] forneceram alguns indícios sobre a formação e a estabilidade do nucleóide bacteriano. Esses autores analisaram cuidadosamente os efeitos das frações protoplasmáticas protéicas ligantes e não ligantes (ao cromossomo) sobre a sedimentação do DNA *in vitro*. Seus resultados mostraram que nem a fração não ligante (mesmo em concentrações nominais 10 vezes maiores que as protoplasmáticas) tampouco a fração ligante eram capazes *per si* de induzir a formação de agregados de DNA. No entanto, conjuntamente, as proteínas ligantes e não ligantes o faziam. Numa série de outros experimentos, nos quais a fração protéica não-ligante foi substituída pelo polímero PEG, resultados semelhantes foram obtidos: o sinergismo entre proteínas catiônicas (ligantes, portanto) e colóides neutros na condensação do DNA *in vitro*.

No artigo 2, discutem-se os resultados obtidos por aqueles autores bem como as bases moleculares que suportam tais resultados ao longo das linhas do modelo proposto por de Vries para condensação de DNA induzida por polímero flexível [15]. Experimentos de espalhamento dinâmico de luz e estudos de sedimentação junto à análise do sobrenadante por meio de eletroforese em gel de agarose são realizados nas soluções contendo o plasmídeo pUC 18 e a proteína catiônica sso7d (que se liga ao DNA) para ilustrar a generalidade dos resultados de Murphy e Zimmermann. O poli (etilenoglicol) é utilizado para mimetizar a fração protoplasmática não ligante [21].

A partir das estimativas obtidas experimentalmente para a concentração crítica do PEG em função da concentração da proteína (em condições fisiológicas i.e., pH=7.0 e concentração molar de NaCl próxima a 150 mM) o digrama de fase da transição é construído.

Uma imagem bastante simples é então proposta para dar suporte aos achados experimentais e a conclusão é assentada com bastante generalidade: para a formação e manutenção do nucleóide procarioto, o sinergismo entre a blindagem eletrostática produzida pela ligação das proteínas catiônicas ao DNA e as interações de depleção induzidas pelos componentes neutros presentes no protoplasma (ou mesmo com carga negativa, o que apenas incrementaria o efeito de depleção) é indispensável. Em outras palavras, *segmentos de DNA de diâmetro efetivo maior e densidade de carga mais baixa que segmentos de DNA não complexados* são muito mais susceptíveis à condensação-ψ que esses últimos.

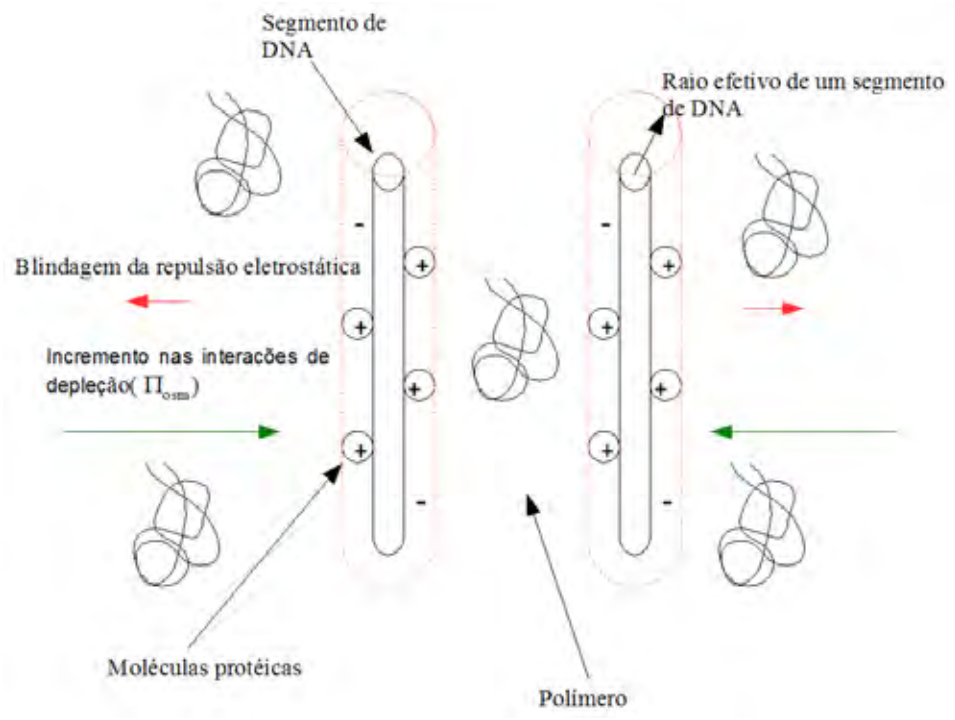

Figura 7 - Representação do colóide DNA/PEG/proteína e das interações dominantes que induzem a transição-ψ (nesse caso, os segmentos de DNA estão complexados a proteínas catiônicas). Os segmentos de DNA são representados pelos segmentos cilíndricos e as proteínas por esferas com carga positiva. As moléculas do polímero flexível são representadas pelas curvas contínuas (conformação “coil-like”).

Artigo 3

Sumário

Na década de 60, Vinograd *et al* abriram um novo capítulo no estudo da conformação da molécula de DNA. Esses pesquisadores inferiram, a partir de estudos de sedimentação do genoma viral (polioma vírus), que o DNA poder-se-ia apresentar numa conformação circular fechada formando super-hélices[22]. Tal conformação, mais compacta que a forma linear correspondente, revelou-se mais comum e geral do que se pensava, sendo que, numa certa medida, o genoma procariótico (*Archaea e Bacteria*), o genoma viral, o genoma mitocondrial e cloroplástico apresentam-se na forma circular fechada com implicações biológicas importante: para citar um exemplo, uma redução mínima na quantidade de super-hélices implica, por exemplo, na não eqüipartição do DNA entre as células bacterianas durante a divisão celular [23, 24].

No contexto da condensação-ψ do DNA, poucos estudos têm enfocado a influência da topologia do DNA e, até certa medida, assume-se implicitamente que a conformação dessa macromolécula (linear, circular aberta ou fechada) não perturba o processo de separação de fases que ocorre entre o polímero neutro e o polímero semiflexível.

No artigo 3 desta tese [25], a condensação-ψ do DNA na forma circular fechada (plasmídeo pUC 18) e na forma linear correspondente (pUC 18 linearizado) são comparadas, valendo-se do fenômeno experimentalmente observado de que a forma condensada do DNA é prontamente sedimentada sob centrifugação, e o sobrenadante analisado por eletroforese em gel de agarose para quantificar a condensação. O que fica claro a partir desse estudo experimental é que o DNA com super-hélices influencia minimante a concentração crítica do poli (etilenoglicol), não obstante a observação de que o PEG_{crit} para a forma circular fechada é sistematicamente maior do que o PEG_{crit} para o DNA linear correspondente.

Estimativas numéricas são feitas comparando as energias livres do DNA na forma dispersa em solução e na forma condensada. Para tal fim, a energia livre do DNA super-helicoidal disperso em solução e na forma condensada são comparadas ao longo das linhas da teoria para condensação de polieletrólitos induzida por polímeros neutros[16]. Nessa teoria, a localização da curva de equilíbrio de fases é obtida igualando-se a energia livre de inserção do DNA *linear* livre em solução ($f_{ins,liv}$) à energia livre de inserção do DNA na *forma condensada* ($f_{ins,cond}$) em uma solução contendo o polímero flexível para uma dada força iônica. A concentração crítica do polímero flexível PEG_{crit} é obtida resolvendo-se a equação $f_{ins,liv} = f_{ins,cond}$.

A energia livre de inserção do DNA linear em uma solução de polímero neutro é calculada multiplicando-se a pressão osmótica da solução pelo volume da molécula de DNA inserida. A fim de se estimar a energia livre de inserção do DNA com super-hélices, devemos levar em consideração que as propriedades termodinâmicas da solução de PEG dependem do comprimento característico das interações dessas moléculas. Comparando-se o diâmetro das super-hélices com o comprimento de correlação da solução de PEG, conclui-se que o primeiro é bem maior que este último sendo a energia livre de inserção do DNA super-helicoildal proporcional ao comprimento de contorno da molécula e dessa forma, as energias livres de inserção do *DNA linear* e *DNA com super-hélices* devem ser aproximadamente iguais em idênticas condições da solução.

Por outro lado, a energia livre de inserção do DNA com super-hélices na forma condensada na solução do polímero flexível pode ser estimada, numa primeira aproximação, assumindo-se que a intensidade das interações entre as super-hélices é aproximadamente igual a do DNA linear ou em

outras palavras, pode-se assumir que o DNA super-helicoidal comporta-se como duas moléculas de DNA *linear aproximadamente paralelas* e separadas pelo diâmetro das super-hélices. Dentro dessas aproximações , nossas estimativas numéricas mostram que a variação da energia mecânica associada as deformações das super-hélices em virtude do confinamente representam apenas uma pequena fração da energia total de interação que é dominada pela forte repulsão eletrostática entre os segmentos das moléculas de DNA e pela energia livre de confinamento dessa molécula no interior do condensado.

A fim de construir uma imagem física mais precisa da conformação das moléculas de DNA circular fechado (DNA com super-hélices) no interior do condensado, simulações de Monte Carlo foram também realizadas. Com efeito, pode-se especular sobre possíveis alterações na conformação do DNA em virtude da forte interação com as demais moléculas no interior do condensado. Eventualmente, poderíamos imaginar o seguinte cenário: a molécula de DNA no interior do condensado tende a se alinhar numa determinada direção (a direção do vetor diretor **n** associado ao campo nemático que mimetiza as interações inter-moleculares) e dependendo da intensidade do campo, parte do "writhe" converter-se-ia em "twist" preservando o "linking number" em virtude da igualdade [26] :

$$Lk = Wr + Tw,$$

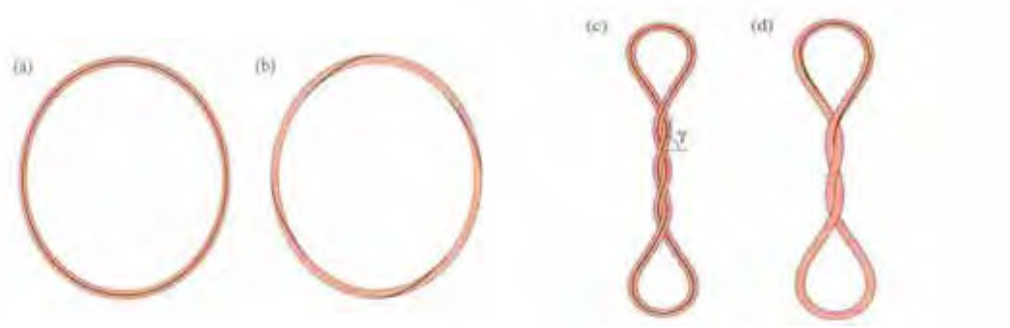

Figura 8 – Ilustração das conformações circular aberta (a) e circular fechada (b) da molécula de DNA por meio de um tubo elástico (curva em vermelho). Na figura b, uma das extremidades da molécula de DNA foi torcida mantendo a outra extremidade fixa, seguida pela ligação das extremidades (a torção da curva preta que representa o eixo da molécula de DNA ilustra a deformação introduzida). Dizemos então que a molécula apresenta " twist" (Tw) ou estresse torcional (Lk =-4 e Tw =-4).Na figura (c) parte to twist foi convertido em wrhite, ou seja, o eixo da super hélice forma uma hélice em volta de si (o wrhite pode ser entendido geometricamente dessa forma). No caso (c) Lk =-4 eWr ≈-4. Na figura (d) o excesso do " linking number Lk" é particionado entre as duas formas: "twist e wrhite". Nesse caso, temos aproximadamente o seguinte particionamente: Tw ≈-1 and Wr≈ -3. (d).O ângulo γ representa o ângulo de curvatura local da molécula de DNA com relação ao eixo da super hélice.

Nas simulações, o modelo do "colocar de contas" é utilizado para representar a molécula de DNA circular fechada e a função Hamiltoniana do sistema possui a seguinte forma:

$$H[\mathbf{r}_1, \mathbf{r}_2, \mathbf{r}_3, \ldots \mathbf{r}_N] = \tfrac{1}{2} k_m \Sigma(\left| (\mathbf{r}_{n+1} - \mathbf{r}_n) \right| - l_b)^2 + \tfrac{1}{2} k_s \Sigma (\arccos(\left| (\mathbf{t}_{n+1} - \mathbf{t}_n) \right|))^2 + 2\pi^2 k_t (\Delta Lk - Wr)^2/N + \Sigma U_{ele}(\left| (\mathbf{r}_{n+1} - \mathbf{r}_n) \right|) + \Delta N [\mathbf{r}_1, \mathbf{r}_2, \mathbf{r}_3, \ldots \mathbf{r}_N]$$

Nesse modelo, *N* esferas são unidas por potencias harmônicos (primeiro termo do Hamiltoniano) e suas coordenadas dadas pelos vetores $[\mathbf{r}_1, \mathbf{r}_2, \mathbf{r}_3, \ldots \mathbf{r}_N]$. Os vetores $\mathbf{t}_n$ são vetores unitários que ligam o centro de duas esferas consecutivas e o mecanismo de persistência é introduzido por um potencial harmônico angular (segundo termo do Hamiltoniano); o terceiro termo representa a

contribuição da energia torcional da molécula e o quarto termo o potencia eletrostático (U_{ele} - potencial de Coulomb blindado na aproximação de Debye-Huckel) entre as esferas. As interações entre moléculas distintas são incluídas em ΔN [$\mathbf{r}_1$, $\mathbf{r}_2$, $\mathbf{r}_3$,…$\mathbf{r}_N$] no qual se consideram simultaneamente a orientação preferencial ao longo do diretor **n** e as interações de depleção (curto alcance) ao nível de dois segmento. Os detalhes da simulação podem ser encontrados no artigo 3[25]. As simulações de Monte Carlo revelam que o cenário anteriormente descrito é bastante improvável e que apenas uma redução sensível no diâmetro do DNA pode ser constatada, em acordo com os achados experimentais de Torbet e Dicapua[27].

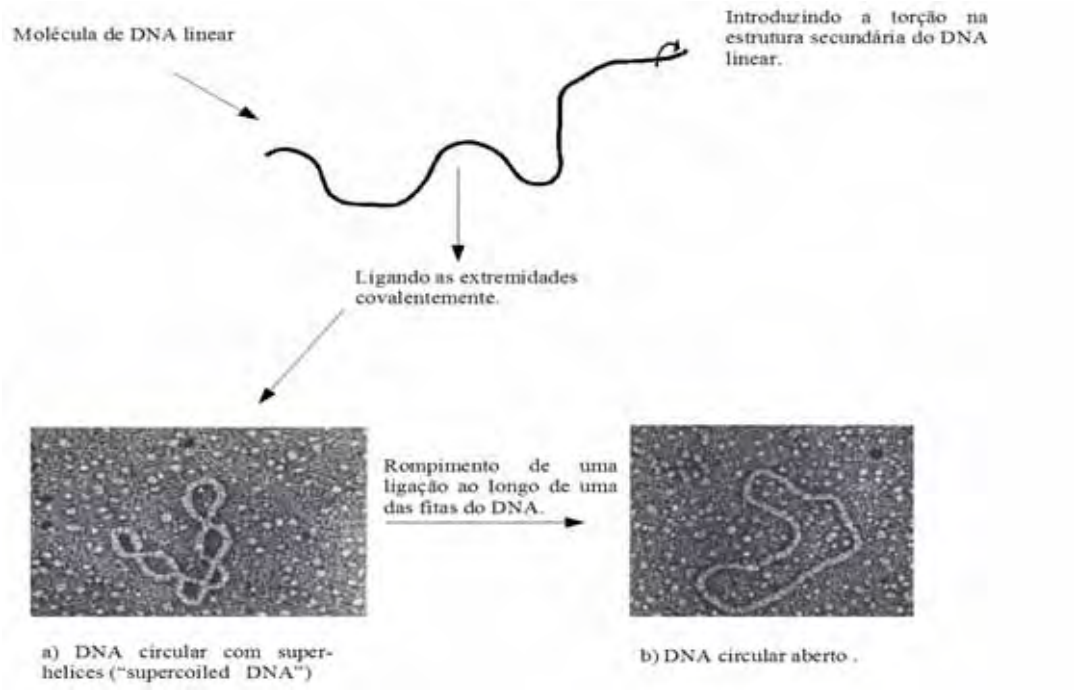

Figura 9 - Ilustração do processo de introdução de torção e conseqüente formação de super- hélices numa molécula de DNA linear. A curva contínua superior representa a molécula de DNA linear (sem torção adicional). A gravura da esquerda é uma eletromicrografia do DNA com super-hélices (pUC18) e a gravura da direita é uma eletromicrografia da forma circular relaxada do DNA (que pode ser obtida ligando-se as extremidades do DNA linear sem introduzir torção ou pela quebra de uma ligação covalente (ligação fosfodiéster) ao longo de uma das fitas da molécula de DNA).

Manuscrito

Sumário

Os resultados experimentais apresentados no capítulo 1[13] encontram uma explicação natural quando as interações de depleção entre o polímero flexível (PEG) e o polieletrólito semi flexível (DNA) são invocadas [17]: em virtude da redução do espaço configuracional, o polímero neutro é depletado da região entre os segmentos do polímero semi flexível. Localmente, então, a concentração do PEG entre os segmentos do DNA é reduzida com relação à concentração do "bulk" da solução. Essa diferença de concentrações implica numa diferença de pressões osmóticas que força à aproximação entre os segmentos de DNA: quando a diferença de pressões osmóticas ultrapassa um valor crítico, superando a repulsão entre segmentos distintos da cadeia de DNA, a molécula de DNA compacta-se e passa a forma condensada.

A dependência observada dos valores críticos de concentração do polímero flexível (PEG) necessárias para induzir a condensação-ψ em função do seu grau de polimerização (N) pode ser entendida em termos estatísticos simples: para um dado volume físico, tanto maior o número de microestados "congelados" da cadeia quanto maior o seu grau de polimerização (N), ou seja, maior a variação de entropia envolvida no processo de inserção de uma molécula de PEG na fase condensada (com relação ao "bulk" da solução). As propriedades mecânico-estatísticas desse processo podem ser quantificadas rigorosamente utilizando-se *a equação de Edwards* para a distribuição de probabilidade $G(\boldsymbol{r},\boldsymbol{r_o},N)$ da distancia "end-to-end" de cadeia polimérica [28]:

$$- l^2_k/6\ \nabla_r^2\ G(\boldsymbol{r},\boldsymbol{r_o},N) + V(\boldsymbol{r})G(\boldsymbol{r},\boldsymbol{r_o},N)\ /K_BT = -\ \partial_N\ G(\boldsymbol{r},\boldsymbol{r_o},N)$$

Partindo-se da função $G(\boldsymbol{r},\boldsymbol{r_o},N)$ pode-se especificar completamente sua termodinâmica e consequentemente descrever as interações entre o PEG e o DNA (ou qualquer outro polímero flexível confinado) determinando-se por exemplo, o potencial químico e a pressão osmótica do polímero confinado.

O segundo ponto importante a ser observado quando tratamos de soluções de polímeros neutros diz respeito à interação entre essas macromoléculas que é significativa mesmo em concentrações relativamente baixas (da ordem 1%) para polímeros de alto peso molecular [29]. Dessa forma, incluir os desvios do comportamento ideal na expansão do virial para as propriedades termodinâmicas da solução é essencial e podem modificar até mesmo qualitativamente o comportamento de fase de tais misturas [30]. Quando o regime assimptótico de alto peso molecular é atingido ($N\rightarrow\infty$) o comportamento universal é bem descrito pela teoria de scaling. Para pesos moleculares baixos, entretanto, a teoria de Flory-Huggins para soluções poliméricas está em melhor acordo com os resultados experimentais. Essas correções são importantes especialmente em concentrações moderadas (regime semi-diluído).

O terceiro aspecto a ser considerado inclui a interação entre os segmentos da cadeia de DNA, assumindo-os como segmentos rígidos dentro da escala de seu comprimento de persistência (50 *nm*). Pode-se incluir, numa primeira aproximação, a repulsão eletrostática como um aumento efetivo no diâmetro desses segmentos (2.4 *nm*) dependente da força iônica da solução: quanto mais baixa a força iônica maior o comprimento característico das interações eletrostáticas e, portanto, maior o volume excluído por um dado segmento aos demais [31].

O comportamento de fase pode ser determinado a partir das condições de equilíbrio termodinâmico: *a*) igualdade dos potenciais químicos de todas as espécies em ambas as fases e *b*) igualdade das pressões osmóticas em ambas as fases. Podem-se estimar, dessa forma, condições em que a mistura é instável e, portanto, o sistema separa-se em duas fases, uma rica em polímero flexível e outra rica em segmentos do polieletrólito.

Uma característica particular das soluções de polímeros neutros diz respeito à estrutura da solução (os comprimentos de escala importantes para a termodinâmica da solução) para regimes de concentração diversos. No regime diluído, o comprimento de correlação característico da solução é o raio de giração do polímero ($R_g \sim N^{3/5}$). À medida que a concentração aumenta (e, portanto a interação entre as moléculas) o comprimento de correlação passa a independer de N (para valores de $N>>1$) sendo função apenas da concentração ($\xi \sim ø^{-3/4}$) [32]. Em concentrações suficientemente elevadas, as forças de depleção são superadas pelas forças que tendem a afastar os segmentos (volume excluído, repulsão eletrostática e pressão exercida pelo PEG no interior da fase condensada) e o condensado redissolve-se, fenômeno observado experimentalmente. Para polímeros de baixo peso molecular que podem adentrar a fase condensada sem grande custo entrópico, os valores críticos da concentração do PEG são relativamente maiores que para PEG de maior peso molecular para induzir a condensação e menores para induzir a descondensação. Ademais, para moléculas suficientemente pequenas do polímero flexível a condensação do DNA não ocorre de maneira alguma, visto não haver particionamento do polímero entre as fases. Todas essas conclusões encontram suporte experimental [13].

Referências Bibliográficas

1 - Cohen Stuart, M.A. *Lectures Notes on Colloid Science* – Laboratório de físico-química e ciências coloidais, Universidade de Wageningen-Holanda. **2007**.
2 - de Vries, R., Cohen Stuart, M.A. – *Curr. Opin. Coll. Inter*.**2006** (11):295-301
3 - Israelachvili,J – *Intermolecular forces and surface forces*- Academic Press.**1991**.
4- Verwey,E.J.W., Overbeek,J.TH.G. *Theory of the stability of liophobic colloids* – Elsevier Publishing Company .**1948**.
5- Asakura,S., Oosawa,F. –*J. Phy. Chem*. **1954**,(22):1225-1226
6- Durbin,S.D.,Feher,G. *Annu.Rev.Phys.Chem.***1996**,47:171-204
7-Odijk,T. – *Biophys.Chem.* **1998**,(73):23-29
8- Lerman, L.S. – *Proc. Natl. Acad. Sci*. **1971**,(68):1886-1890
9- Rau,D.C., Lee,B., Parsegian,V.A. – *Proc. Natl. Acad. Sci*. **1984**,(81):2621-2625
10- Odijk,T. – *Macromolecules*. **1983**,(16):1340-1344
11- Odijk,T. – *Biophys.Chem*. **1993**,(46):69-75
12- Jordan,C.F., Lerman,L.S., Venable,J.H. – *Nature New Biology*. **1972**,(236):67-70
13- Ramos, J.E.B,Jr., de Vries,R., Neto,J.R. – *The J. Phys. Chem. B*. **2005**,(236):67-70
14-Vasilevskaya, V.V.,Khohholov,A.R.,Matsuzawa,Y., Yoshikawa,K. *The J. Phys. Chem. B*. 199**5**, (102):6595-6661
15-Grosberg,A.Yu.,Erukhimmovitch,I.Ya.,Shakhnovitch,E.I.– Biopolymers.1982,(21):2413-2432
16-de Vries,R. – *Biophy. J*.**2001**,(80):1186-1194
17- Ramos, J.E.B,Jr (manuscript).
18- Hoog,S. *Essential Microbiology*- John Wiley and Sons,ltd **2005**
19- Zimmerman, S.B. *J. Struc. Biol*.**2006**, (156): 255-261
20- Murphy,L.D., Zimmerman, S.B. *Biophys.Chem*. **1995**,(57):71-92
21- Ramos, J.E.B,Jr., Wintraecken,K., Geerling,A., de Vries,R. *Biophy. Rev. Let*. **2007**,(2)259:265.
22 - Vinograd,J.,Lebowitz,J., Radolf,R., Watson,R.,Laipis,P. *Proc. Natl. Acad. Sci*. **1965**,(53):1104-1108.
23- Lodish,H *et a*l. *Biologia Celular e Molecular*. 5ª Edição-Editora Artmed
24- Sawitzke,J.A., Austin,S.*Proc. Natl. Acad. Sci.* **1999**,(97):1671-1676.
25- Ramos, J.E.B,Jr., Neto,J.R., de Vries,R. *The J.Chem.Phys.* **2008** (129):185102-1-6
26-Bates,A.D., Maxwell,A. *DNA Topology*. Oxford University Press **1993**.
27- Torbet,J., Dicapua,E. *EMBO J.* **1989**, (8):4351-4355
28- Doi,M., Edwards,S.F. *The Theory of Polymer Dynamics* – Claredon Press-Oxford **1986**.
29-Abbot,N.L., Blankstein,D., Hatton,T.A. *Macromolecules*. **1992**,(25-3):3932-3941
30-Castelnovo,M., Gelbart,W.M. *Macromolecules*.**2004**,(37):3510-3517
31- Odijk,T. *J Poly.Sci*. **1978**, (16):627-639
32- de Gennes,P.G. *Scaling Concepts in Polymer Physics*- Cornell University Press **1979**

DNA Ψ-Condensation and Reentrant Decondensation: Effect of the PEG Degree of Polymerization

José Ésio Bessa Ramos, Jr.,[†] Renko de Vries,[‡] and João Ruggiero Neto*[,†]

Department of Physics, IBILCE UNESP, Universidade Estadual Paulista, R. Cristóvão Colombo 2265, 15054-000 São José do Rio Preto SP, Brazil, and Laboratory of Physical Chemistry and Colloid Science, Department of Agrotechnology and Food Sciences, Wageningen University, P. O. Box 8038, 6700 EK, Wageningen, The Netherlands

Received: May 23, 2005; In Final Form: October 6, 2005

ψ-Condensation of DNA fragments of about 4 kbp was induced by poly(ethylene glycol) (PEG), with degrees of polymerization ranging from 45 to 182, and univalent salt (NaCl). Using circular dichroism spectroscopy, we were able to accurately determine the critical amount of PEG needed to induce condensation, as a function of the NaCl concentration. A significant dependence on the PEG degree of polymerization was found. Phase boundaries determined for the multimolecular condensation were very similar to those observed previously for the monomolecular collapse, with two asymptotic regimes at low and high salt concentrations. We analyze our data using a theoretical model that properly takes into account both the polyelectrolyte nature of the DNA and the liquid crystallinity of the condensed phase. The model assumes that all PEG is excluded from the condensates and shows reentrant decondensation only at low salt. We also systematically study reentrant decondensation and find a very strong dependence on PEG molecular weight. At low PEG molecular weight, decondensation occurs at relatively low concentrations of PEG, and over a wide range of salt concentrations. This suggests that in the reentrant decondensation the flexible polymers used are not completely excluded from the condensed phase.

Introduction

DNA undergoes a transition from a disperse isotropic solution to a liquid-crystalline phase by the addition of flexible polymer and simple salt. The condensed phase, discovered three decades ago,[1] has been called ψ-DNA.[2]

Monomolecular collapse and multimolecular condensation[3,4] are induced by the same physicochemical conditions. For long DNA molecules, in very dilute solutions ($\ll$1 mg/ml), monomolecular collapse dominates,[5] whereas, for shorter DNA molecules and at higher concentrations, multimolecular condensation predominates.

Multimolecular ψ-condensation has been observed for a broad range of DNA contour lengths (10^2−10^4 bp), with DNA concentrations $\ll$1 mg/mL.[6] Multimolecular DNA condensates have been shown to present an anomalous intense differential absorption of circularly polarized light.[2,6,12] The anomalous circular dichroism (CD) spectra are attributed to the supramolecular chiral organization:[6] in the condensed phase, the DNA molecules are tightly packed in planes which are twisted, forming a superhelical structure that preserves a positional ordering similar to a cholesteric phase.[6,12] The CD spectrum is indeed similar to that observed for the highly concentrated DNA cholesteric liquid-crystalline form.[7]

Multimolecular DNA condensation is very similar to monomolecular DNA condensation: for instance, both multimolecular condensed and monomolecular collapsed DNA can, under some conditions, be resolubilized (reentrant decondensation) by further addition of neutral polymer.[5] Also, for very dilute solutions of highly polymerized DNA, both multimolecular condensation and monomolecular collapse were observed to be strongly dependent on the concentrations of poly(ethylene glycol) (PEG) and salt.[5,8]

Phase boundary diagrams, that correlate critical PEG and salt concentrations to induce ψ-DNA, in dilute DNA solutions, were previously obtained for T4 DNA by Vasileviskaya et al.[5] and calf thymus and λ phage DNA by Frisch and Fesciyan.[8] For T4 DNA collapse, it was observed that these diagrams were dependent on the PEG degree of polymerization.[5] Experimental data on reentrant decollapse for highly polymerized DNA are, however, limited to a very restricted range of concentrations and degrees of polymerization of PEG.[5]

Frisch and Fesciyan[8] and Vasylevskaya et al.[5] also present theoretical models, based on Flory−Huggins polymer theory. However, such theories neglect the liquid-crystalline nature of ψ-DNA and do not explicitly include the strong and salt-dependent electrostatic repulsion between neighboring DNA strands in ψ-condensates.

Recently,[9,10] Castelnovo et al. have emphasized the role of correlations between depletion agents in determining the phase boundary for condensation. Under the simplifying assumption that all depletion agent is excluded from DNA condensates, one of us[11] proposed a model for condensation that explicitly takes into account the polyelectrolyte nature of the DNA as well as the liquid-crystalline nature of the condensates. The model quantitatively describes the salt dependence of the critical concentration of depletion agent as measured for the monomolecular transition.[5,8] The model should also be appropriate to describe the multimolecular condensation, but for this case, no systematic experiments have yet been performed on the salt

* Corresponding author. Phone: 550172212240. Fax: 550172212247. E-mail: joao@ibilce.unesp.br.
† Universidade Estadual Paulista.
‡ Wageningen University.

10.1021/jp0527103 CCC: $30.25
Published on Web 11/17/2005

dependence of the critical concentration for both condensation and reentrant decondensation.

Therefore, in the present work, we report experimental phase diagrams (flexible polymer vs salt concentrations) for multimolecular ψ-DNA condensation and compare them with the previously proposed model.[11] The transition is induced by poly(ethylene glycol) (PEG) of four different degrees of polymerization and sodium chloride. We use micromolar concentrations of DNA fragments, about 4 kbp, conditions for which multimolecular condensation predominates. The critical PEG and salt concentrations, both for condensation and reentrant decondensation, are found to sensitively depend on the degree of polymerization of PEG. Whereas the previous model[11] is consistent with the data for condensation, it cannot fully explain the decondensation transition. Possible reasons for this are discussed.

Materials and Methods

Highly polymerized calf thymus DNA, purchased from Pharmacia, was dissolved in 100 mM NaCl at 4 °C overnight. Deproteinization of the DNA was done repeatedly with phenol, phenol−chloroform, and chloroform extraction followed by a series of dialysis against a solution of 100 mM NaCl. This stock solution was sonicated, with a Virsonic model 475 (Virtis Co., New York) cell disruption sonifier. The sonication procedure was the following: 10 mL of DNA solution in a centrifuge tube was sonicated with a tip immersed 3 cm, applying pulses of 30 s at 0 °C followed by interruptions of 30 s at the same temperature. The total sonication times were 5 min. The average fragment length was determined by agarose gel electrophoresis and was about 4 ± 0.5 kbp. The DNA concentrations were determined spectrophotometrically using an extinction coefficient of $\epsilon_{260} = 6600\ M^{-1}\ cm^{-1}$. The ratio A_{260}/A_{280} was found to be equal to 1.88.

The flexible polymers—poly(ethylene glycol) (PEG) with molecular weights (MWs) of 2000, 3350, 6000, and 8000 and with degrees of polymerization (DPs) of 45, 76, 136, and 182, respectively—were purchased from Sigma and were used without further purification.

In our experiments, we first dissolve the PEG in a solution of a given NaCl concentration and then slowly add the DNA. The DNA final concentration was estimated to be equal to 40 mM (in base pairs), around 0.0265 mg/mL. Samples were gently agitated for 20 min and then left to equilibrate for 2 h. All solutions were prepared with doubly distilled and deionized water with an electrical conductivity of 0.6 mS.

The phase transition from a disperse solution to the condensed ψ-phase was monitored by circular dichroism spectroscopy using a Jasco J710 spectropolarimeter. The critical concentration of the flexible polymer, w_{cr}, was defined as the minimum concentration necessary to produce ψ-like spectra. The baseline (PEG and salt solution) was subtracted from all spectra.

Results

DNA Condensation. Figure 1 shows the CD spectra of a 40 mM DNA solution in 0.2 M NaCl to which different amounts (w/w %) of PEG 2000 were added. At 19% PEG, the CD spectra show a positive band centered at 275 nm and a negative band at 240 nm, characteristic of a disperse solution of the B conformation of DNA. Increasing the PEG concentration to 20% resulted in a 10 times more intense and nonconservative spectrum, with a broad negative band displaced to 270 nm and a slightly positive band above 300 nm. This spectrum is characteristic for ψ-DNA.[12] Further addition of PEG to 22% leads to the reduction of negative band intensity, and the spectrum returns to that of the usual B conformation, indicating a process of reentrant decondensation; see below.

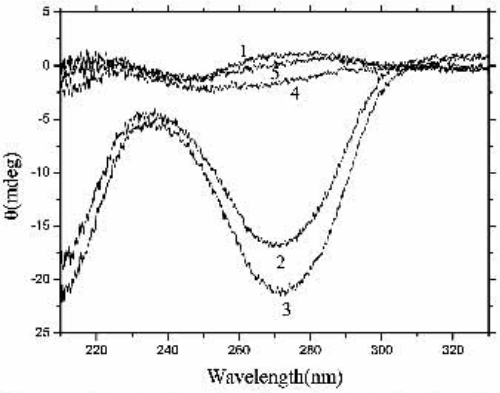

Figure 1. CD spectra for condensation and reentrant decondensation of B-DNA in 0.2 M NaCl induced by PEG 2000. The spectra numbered 1−5 correspond to the following concentrations of PEG: 19% (1), 20% (2), 21% (3), 22% (4), and 23% (5).

With the sample preparation as described here, after 2 h of equilibration, the condensed phase is reasonably stable, judging from the stability of the CD spectra over several hours, and the CD spectra are well reproducible. We have found this experimental approach to be very suitable to obtain a phase diagram for the transition of dispersed DNA to ψ-DNA as a function of the concentrations of salt and flexible polymer.

The phase boundaries for condensation are shown in Figure 2a for PEG with four different molecular weights: 2000, 3350, 6000, and 8000. The critical PEG, w_{cr}, and salt (NaCl) concentrations refer to the minimal concentrations that induce the spectral change from the B conformation to the nonconservative ψ characteristic CD spectrum. In Figure 2b, the phase boundaries obtained for collapse of T4[5] and condensation of calf thymus DNA,[8] induced by PEG with DPs of 200 and 160, respectively, are displayed with our data for PEG with a DP of 182. The w_{cr} versus [NaCl] plots exhibit a similar dependence on salt as observed for the monomolecular collapse or multimolecular condensation with high and low molecular weight DNA. Despite the different experimental approaches and the PEGs used to obtain the plots of Figure 2b, the comparison of these data suggests weak dependence on the DNA molecular weight in the transition to the ψ-phase, in very good agreement with the theoretical model.[11]

The plots in Figure 2 indicate that, at a given flexible polymer concentration, the critical salt concentrations needed for condensation increase with a decrease of the PEG molecular weight. Or, at a fixed salt concentration, the amount of PEG needed to induce condensation increases with a decrease of the PEG molecular weight. In agreement with previous data, we also find two distinct regimes: a low salt and a high salt regime. At low salt, DNA condensation strongly depends on the PEG concentration, whereas, at high salt, it does not.

DNA Decondensation. As shown in Figure 1, increasing the flexible polymer concentration beyond that needed to condensate the DNA leads to decondensation of the DNA (at least for the systems that we study here). Reentrant decondensation has also been observed for the monomolecular DNA collapse.[5] These authors observed reentrant behavior for PEG 20000 (DP = 454) but not for PEG 8200 (DP = 186). Unfortunately, they did not

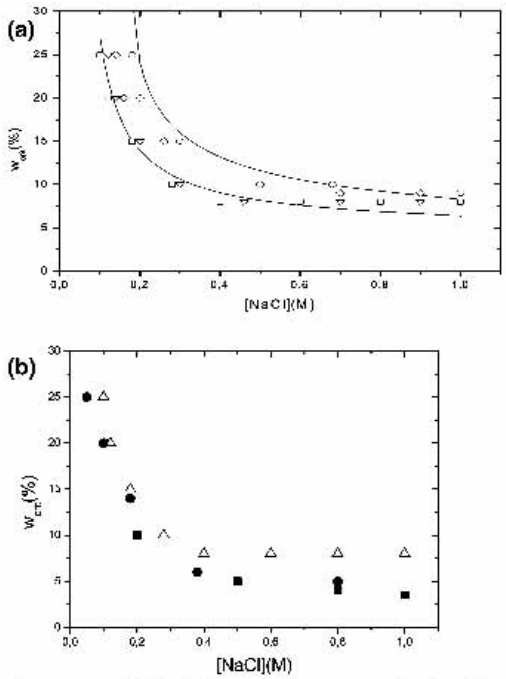

Figure 2. (a) Critical PEG concentration, w_{crit}, as a function of the monovalent salt concentration [NaCl] for different degrees of polymerization of the flexible polymer: PEG 2000 (circles), PEG 3350 (diamonds), PEG 6000 (triangles), and PEG 8000 (squares). The curves are fits to the theoretical model discussed in the text. For clarity, only the fits for PEG 2000 and PEG 8000 are shown. (b) Critical PEG concentration, w_{crit}, as a function of the monovalent salt concentration [NaCl] for T4 DNA[5] with DP = 200 PEG (closed circles), calf thymus DNA[8] with DP = 160 PEG (closed squares), and sonicated calf thymus DNA fragments of 4 kbp with DP = 182 PEG (open triangles, this work).

perform a systematic study of reentrant decollapse as a function of the salt concentration and PEG molecular weight.

While we have observed that all the PEGs that we have used cause decondensation at some polymer concentrations, we have investigated the salt dependence of the decondensation transition only for the lower and higher DP values. Phase boundaries for the condensation and decondensation transition for the two PEG molecular weights, as a function of the salt concentration, are shown in Figure 3. For both PEG molar weights, the hatched region indicates the condensed phase. Outside of this region, the DNA solution does not present ψ-DNA spectra and most probably is a disperse solution.

For most of the decondensation experiments, the concentration of PEG was increased until decondensation was observed. We have also done a few experiments in which we increased the salt concentration at a fixed concentration of PEG. The two procedures gave identical results for the decondensation phase boundaries, suggesting that thermodynamic equilibrium has indeed been attained.

For the high PEG molecular weight, PEG 8000 (DP = 182), we find that reentrant decondensation only occurs at rather high PEG concentrations. We cannot fully explain why Vasilevskaya et al. do not find reentrant decondensation for PEG 8000.

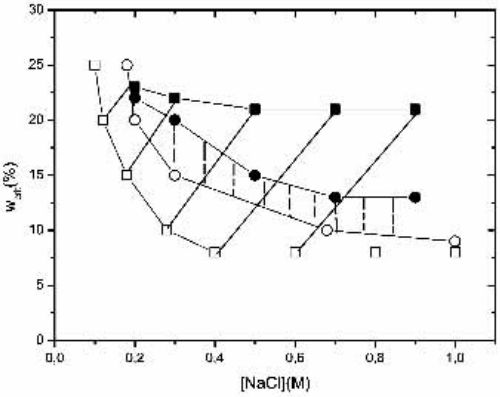

Figure 3. Critical PEG concentration, w_{crit}, as a function of the monovalent salt concentration [NaCl] for condensation (open symbols) and reentrant decondensation (closed symbols) of B-DNA in two different degrees of polymerization of the flexible polymer: PEG 2000 (circles) and PEG 8000 (squares).

Possibly, reentrant decondensation is much more sensitive to the DNA size and concentration than condensation.

For PEG 2000 (DP = 45), reentrant decondensation can occur at much lower concentrations. For this molecular weight, the region of PEG concentrations where condensates are formed is already rather narrow. This result suggests that there might be a minimum degree of polymerization for the flexible polymer to induce ψ-condensation for low molecular weight DNA. The existence of a minimum molecular weight of flexible polymers to achieve DNA condensation was first proposed on theoretical grounds.[13] Kleideter et al.[14] found that even PEG with a molar weight of 900 can still condense DNA. However, we did not observe condensation for PEG 900 at the same salt concentration of their experiments for PEG changing from 10 to 25% in 40 μM DNA (data not shown). Kleideter et al. used DNA fragments of about the same size (3.3 kbp) but at a concentration that was more than 10 times higher than the one we are using here; hence, most likely, under these conditions, the DNA concentration also starts playing an important role.

Condensation Theory. We first briefly review our previous theory.[11] To estimate the location of the phase boundary, the work $f_{ins,free}$ to insert a free DNA chain in a solution containing PEG and salt (per unit length of DNA) is compared with the work $f_{ins,cond}$ to insert the same DNA but in the condensed form (again per unit length of DNA). Critical PEG and salt concentrations are estimated by equating these two free energies:

$$f_{ins,free} = f_{ins,cond} \quad (1)$$

The work $f_{ins,free}$ of inserting free DNA in a solution of inert flexible polymers (per unit length of DNA; polymer weight fraction, w) is estimated from polymer scaling theory:

$$f_{ins,free} = \mu_1 w + \mu_2 w^{9/4} \quad (2)$$

The expression involves two numerical constants, μ_1 and μ_2, that depend on the properties of the flexible polymer but not on its concentration.

The work $f_{ins,cond}$ of inserting DNA in the condensed state has two contributions: that of assembling, or packing, the condensate and the osmotic work of inserting the assembled

TABLE 1: Numerical Constants Used in the Interpolation Formula for the PEG Osmotic Pressure

	a	*b*	*c*
PEG 2000	4.64	0.18	0.67
PEG 3350	3.74	0.57	0.44
PEG 6000	4.12	0.28	0.59
PEG 8000	2.96	0.95	0.36

condensate into the solution of flexible polymers:

$$f_{\text{ins,cond}} = f_{\text{pack}} + \frac{3^{1/2}}{2}\Pi d^2 \qquad (3)$$

The packing free energy, f_{pack}, is the free energy (per unit length) of transferring DNA from a dilute solution into a liquid-crystalline phase. This term is calculated using the self-consistent field model of Odijk,[15] which takes into account the electrostatic repulsion between neighboring DNA molecules in a hexagonal array as well as the loss of configurational entropy due to confinement. The second contribution is the osmotic work of inserting the condensate, where Π is the osmotic pressure and d is the center-to-center distance of neighboring parallel DNA molecules in the condensate.

We obtained the best fits to the experimental phase diagrams for the four different PEGs by using a unique value for μ_2 of 102 k_BT/nm. The μ_1 values used in these fits were 8.0, 6.5, 5.2, and 4.1 k_BT/nm for PEG 2000, 3350, 6000, and 8000, respectively. The fits for PEG 2000 and PEG 8000 are shown, together with the experimental data, in Figure 2. In calculating the phase boundaries, the osmotic pressure at each PEG concentration and molecular weight was estimated using the interpolation formula published previously.[16]

$$\log(\Pi(\text{Pa})) = a + b(100w)^c$$

where w is again the polymer weight fraction. Values for the numerical constants a, b, and c are listed in Table 1. A plot of the value of μ_1 as a function of the degree of polymerization of the flexible polymer is shown in Figure 4. Polymer scaling theory suggests $\mu_1 \sim N^{-1}$ while μ_2 should be roughly independent of the degree of polymerization, N, of the PEG. Indeed, the experiments show a decreasing value of μ_1, but we cannot test the scaling predictions here, in view of the rather low values and limited range of the molecular weights.

The parameters μ_1 and μ_2 obtained in best fitting the theoretical curves to the experimental data allow us to estimate the force resisting insertion of the DNA into a PEG solution. This force equals the work $f_{\text{ins,free}}$ of inserting free DNA into a PEG solution (per unit length of DNA). There has been quite some interest in this force, in view of recent experiments on virus capsids ejecting their DNA into PEG solutions.[17] Recently, this force was calculated,[9] and expressions similar to that of de Vries[11] were derived, except for an added term representing the contribution of surface tension at high concentrations of flexible polymer. From our data, we find a force of around 20 pN, for a PEG solution with an osmotic pressure of 10 atm. This force is somewhat higher than the values measured.[17]

Reentrant decollapse was also found, for some parameter values, in the previously proposed model.[11] However, the region of reentrant decollapse in this model is restricted to a narrow zone of salt concentrations, close to the salt concentration below which the critical PEG concentration for condensation starts to increase rapidly (from approximately 0.1 to 0.3 M). The physical picture suggested in that model[11] is that, at low salt, higher pressures (and hence higher PEG concentrations) are needed to stabilize the condensates. These correspond to smaller values

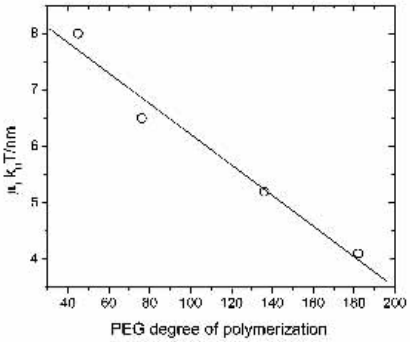

Figure 4. μ_1 vs PEG DP μ_1 values obtained from the best fitting of the condensation phase diagrams.

of the correlation length,[18] ξ, of the semidilute flexible polymer solution (for values for PEG, see ref 18). Below some ionic strength, the correlation lengths, ξ, are smaller than the lattice spacings, d, of the condensates, and the flexible polymer enters and redisolves the condensate.

The model of de Vries assumes full exclusion of PEG from the condensates. From the work of Parsegian et al.,[19] it is known that this is indeed reasonable at somewhat higher PEG molecular weights. However, the PEG molecular weights used here are rather low, and the corresponding polymer coils are rather small. For this case, it is no longer clear that all PEG will be excluded from the condensates. This might explain the discrepancy between the experimental phase boundaries for decondensation at low PEG molecular weight found here and the model of de Vries.

It might be possible to address the salt dependence of the decondensation transition using the approach proposed recently,[10] which is more general and does not assume full exclusion of depletion agent from the condensates. This, however, would imply a neglect of the liquid-crystalline nature of the condensates. To do better, one first would need to address the theoretical problem of small flexible polymer coils confined inside liquid-crystalline DNA.

Concluding Remarks

Multimolecular condensation of short DNA molecules by PEG is very similar to the monomolecular collapse of long, single DNA molecules induced by PEG. Condensation, but especially decondensation, is rather sensitive to the PEG molecular weight. Assuming full exclusion of PEG from the condensates leads to an adequate theoretical description of the condensation phase boundaries (critical PEG concentration versus salt concentration) but not of the decondensation phase boundaries. It seems that under conditions of decondensation it is imperative to take into account the fact that the depletion agent may also enter the condensates.

Acknowledgment. This work was supported in part by CAPES and FAPESP Brazilian agencies.

References and Notes

(1) Lerman, L. S. *Proc. Natl. Acad. Sci. U.S.A.* **1971**, *68*, 1886.
(2) Jordan, C. F.; Lerman, L. S.; Venable, J. H., Jr. *Nat. New Biol.* **1972**, *236*, 67.
(3) Bloomfield, V. A. *Curr. Opin. Struct.. Biol.* **1996**, *6*, 334.
(4) Sikorav, J.-L.; Pelta, J.; Livolant, F. *Biophys. J.* **1994**, *67*, 1387.

(5) Vasilevskaya, V. V.; Khokholov, A. R.; Matsuzawa, Y.; Yoshikawa, K. *J. Chem. Phys.* **1995**, *102*, 6595.
(6) Bustamante, C.; Samori, B.; Builes, E. *Biochemistry* **1991**, *30*, 5661.
(7) Livolant, F.; Maestre, M. F. *Biochemistry* **1988**, *27*, 3056.
(8) Frisch, H. L.; Fesciyan, S. *J. Polym. Sci., Polym. Lett. Ed.* **1979**, *17*, 309.
(9) Castelnovo, M.; Bowles, R. K.; Reiss, H.; Gelbart, W. M. *Eur. Phys. J. E* **2003**, *10*, 191.
(10) Castelnovo, M.; Gelbart, W. M. *Macromolecules*. **2004**, *37*, 3510.
(11) de Vries, R. *Biophys. J.* **2001**, *80*, 1186.
(12) Keller, D.; Bustamante, C. *J. Chem. Phys.* **1986**, *84*, 2972.
(13) Grosberg, A. Y.; Erukhmovitch, I. Y. Shakhnovitch, E. I. *Biopolymers* **1982**, *21*, 2413.
(14) Kleideter, G.; Nordmeir, E. *Polymer* **1999**, *40*, 4025.
(15) Odijk, T. *Biophys. Chem.* **1993**, *46*, 69.
(16) Parsegian, V. A.; Rand, R. P.; Rau, D. C. *Methods Enzymol.* **1995**, *259*, 43.
(17) Evilevitch, A.; Castelnovo, M.; Knobler, C. M.; Gelbart, W. M. *J. Phys. Chem. B* **2004**, *108*, 6838.
(18) Abbot, N. L.; Blankschtein, D.; Halton, T. A. *Macromolecules* **1991**, *24*, 4349.
(19) Parsegian, V. A.; Rand, R. P.; Rau, D. C. *Methods Enzymol.* **1986**, *127*, 400.

Biophysical Reviews and Letters, Vol. 2, Nos. 3 & 4 (2007) 259–265

SYNERGY OF DNA-BENDING NUCLEOID PROTEINS AND MACROMOLECULAR CROWDING IN CONDENSING DNA

ESIO BESSA RAMOS

Department of Physics, IBILCE UNESP,
Universidade Estadual Paulista,
R. Cristóvão Colombo 2265, 15054-000,
São José do Rio Preto SP, Brazil

KATHELIJNE WINTRAECKEN

Laboratory of Physical Chemistry and Colloid Science,
Wageningen University, P. O. Box 8038,
6700 EK, Wageningen, The Netherlands
Kathelijne.Wintraecken@wur.nl

ANS GEERLING

Laboratory of Microbiology, Wageningen University,
Dreijenplein 10, 6703 HB Wageningen, The Netherlands
Ans.Geerling@wur.nl

RENKO DE VRIES

Laboratory of Physical Chemistry and Colloid Science,
Wageningen University, P. O. Box 8038,
6700 EK, Wageningen, The Netherlands
Renko.deVries@wur.nl

Received 8 January 2008

Many prokaryotic nucleoid proteins bend DNA and form extended helical protein-DNA fibers rather than condensed structures. On the other hand, it is known that such proteins (such as bacterial HU) strongly promote DNA condensation by macromolecular crowding. Using theoretical arguments, we show that this synergy is a simple consequence of the larger diameter and lower net charge density of the protein-DNA filaments as compared to naked DNA, and hence, should be quite general. To illustrate this generality, we use light-scattering to show that the 7kDa basic archaeal nucleoid protein Sso7d from *Sulfolobus solfataricus* (known to sharply bend DNA) likewise does not significantly condense DNA by itself. However, the resulting protein-DNA fibers are again highly susceptible to crowding-induced condensation. Clearly, if DNA-bending nucleoid proteins fail to condense DNA in dilute solution, this does not mean that they do not contribute to DNA condensation in the context of the crowded living cell.

Keywords: DNA condensation; DNA-protein interactions; macromolecular crowding.

1. Introduction

The effect of nucleoid proteins on the global gene expression in prokaryotic cells is now well established[1] but their role in nucleoid compaction is less clear. For example, many of the most abundant prokaryotic nucleoid proteins introduce bends in DNA. When complexed with DNA at appreciable coverage, helical protein-DNA filaments are formed that are typically extended rather than condensed. This has been shown, for example, for bacterial HU from *E. coli* using AFM and single-molecule force measurements[2,3] and for archaeal Sac7d from *Sulfolobus acidolaricus* using small angle X-ray scattering.[4]

On the other hand, Murphy and Zimmerman[5] find that *E. coli* HU strongly promotes crowding induced DNA condensation (induced by adding flexible polymers or non-binding proteins such as serum albumin or bacterial cytoplasmic proteins). This effect is especially strong at the high HU concentrations for which it has been suggested[2,3] that HU should counteract DNA compaction.

Why are extended helical HU-DNA filaments so much more susceptible to crowding induced condensation? Here we wish to explain the molecular basis for this somewhat unexpected synergy in terms of a simple theory that we previously developed for polymer-induced condensation of semiflexible polyelectrolytes.[6] We also briefly comment on the relation between this phenomenon and the formation and stability of prokaryotic nucleoids.

To complement the previous results on *E. coli* HU, and to illustrate the generality of the phenomenon, we also study crowding-induced condensation of extended protein-DNA filaments for another well characterized DNA bending nucleoid protein: archaeal Sso7d from *Sulfolobus solfataricus*. This protein, and the nearly identical Sac7d from *Sulfolobus acidolaricus* have been shown to non-specifically introduce sharp bends into double stranded DNA. At higher concentrations, they fully cover DNA at about one protein per 4bp, and form extended helical filaments.[4]

2. Materials and Methods

2.1. *Protein expression and purification*

The protein Sso7d was overexpressed in *E. coli* (DE3)pLysS, harboring the plasmid pET-3b/*sso7d*, described before.[7] Pelleted cells from 1.5 L culture were suspended in 15 ml of suspension buffer: 30 mM Na_2HPO_4-HCl, 500 mM NaCl, pH 6.5. Cells were lysed using a French press (3 times at 1000 psi) and centrifuged for 50 min at 12,000 g, 4°C. To remove the majority of *E. coli* proteins, the supernatant was heated to 80°C for 40 min, centrifuged for 2 hours at 45,000 g at 4°C, and filtered using a 0.45 μm pore size syringe filter. After a concentration step, we exchanged buffer using disposable PD10 columns, to buffer A: 30mM Na_2HPO_4-HCl, pH 6.5. The suspension was loaded onto a MonoS column, equilibrated with buffer A, and eluted with a linear NaCl gradient (0...0.6 M). Sso7d eluted at around 0.35 M. No other bands were detected on SDS-PAGE for fractions in the peak center, but

some minor contaminations of around 15kDa were detected for the fractions further away from the peak center. These fractions were pooled and concentrated, applied to a Superdex 75 column, and eluted with buffer A, after which SDS-PAGE showed only a single band corresponding to Sso7d. Purified protein was exchanged to storage buffer (20 mM Tris-Hcl pH 7.7, 1 mM EDTA, 20% glycerol, 200 mM NH_4Cl, 200 ppm NaN_3, 200 ppm β-mercaptoethanol) using PD10 columns, concentrated to about 3 mg/ml and stored at $-4°C$. Protein concentrations were determined by UV spectrophotometry using[4] $\varepsilon_{278} = 1.1\,\mathrm{mL/(mgcm)}$.

2.2. *DNA purification*

Plasmid pUC18 (2686 bp) was isolated from *E. coli* using Qiagen Kits according to the instructions of the manufacturer, and linearized using EcoRI.

2.3. *Light scattering*

Light-scattering was measured at 25°C using a Malvern NanoS, operating at a wavelength of 633 nm and a scattering angle of 173°. The effective hydrodynamic radius reported is the peak position of the monomodal distribution fit as reported by the Malvern DTS software, version 5.0. Absolute scattering intensities were calculated using toluene as a standard. For all of the experiments, concentrated stock DNA was diluted in 10 mM Tris-HCl buffer, pH 7.0, 150 mM NaCl. The final DNA concentration in the experiments was 12 μg/ml, as determined using UV spectrophotometry. Protein concentrations ranged from 0 to 1 protein per DNA basepair.

2.4. *Condensation assay*

The condensation assay that was used is similar to that of Murphy and Zimmerman.[5] Protein-DNA complexes are equilibrated with flexible polymer solutions (final DNA concentration and buffer conditions as in the light-scattering experiment), centrifuged at 13000 g for 1 hour and the supernatant is analyzed using agarose gel-electrophoresis. Condensation is observed as a decreased, and ultimately vanishing intensity for the DNA bands in the agarose gels.

3. Results and Discussion

To demonstrate that Sso7d indeed does not condense DNA in free solution at physiological ionic strength, as was shown previously for the nearly identical Sac7d using small angle X-ray scattering, we have performed static and dynamic light-scattering measurements on complexes with 2686 bp long pUC18 DNA, linearized with EcoRI. The effective hydrodynamic radius and scattered intensity as a function of protein/DNA molar ratio are shown in Fig. 1. The static scattering closely follows the extent of binding since free proteins hardly contribute to the scattering.

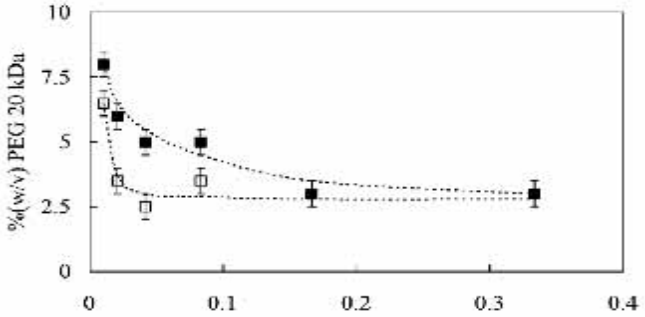

Fig. 3. Condensation assay. Estimated concentration of polymer (PEG 20 kg/mol) at which DNA concentration in the supernatant (after centrifuging for 1 hour at 13,000 g) starts decreasing (open symbols), resp. concentration of polymer beyond which no DNA is detected anymore in the supernatant (closed symbols) using agarose gel electrophoresis.

critical conentration of PEO, the concentration of DNA-Sso7d complexes in the supernatant (after centrifugation) starts decreasing; after a second critical concentration of PEO, no more DNA-Sso7d complexes are detected.

Figure 3 shows our estimates for the two critical PEO concentrations as a function of the protein/DNA ratio. Condensation of EcoRI linearized pUC18 without Sso7d occurs in a rather narrow window around 8% (w/v) of PEO. Increasing the Sso7d/DNA ratio, the amount of PEO needed for condensation decreases rapidly. At low protein concentrations, the transition regime is rather broad, but beyond saturation, the transition becomes very sharp again and occurs at around 3% of PEO.

Previously, we have developed simple analytical estimates for the (ionic strength-dependent) amount of flexible polymer needed to condense semiflexible polyelectrolytes such as DNA and F-actin filaments.[6] These estimates, which assume all polymer is excluded from the condensates, can also be applied to the protein-DNA filaments that we study here. The idea is to compare the free energies (or chemical potentials) of inserting semiflexible polyelectrolytes in solutions of flexible polymers in resp. the free and condensed form. Insertion of free (i.e. uncondensed or extended) semiflexible polyelectrolytes can be dealt with using polymer scaling theory. Per unit length of semiflexible polymer:

$$f_{\mathrm{ins,free}} \approx \mu_1 w + \mu_2 w^{9/4}, \tag{1}$$

where w is the polymer weight concentration (%w/v), and μ_1 and μ_2 are numerical prefactors that depend on the radius a of the semiflexible polyelectrolyte. When inserting a condensate, one has to first push away the flexible polymers (osmotic work) to create space for the condensate and then to assemble the condensate inside this space (packing energy):

$$f_{\mathrm{ins,cond}} \approx f_{\mathrm{osm}} + f_{\mathrm{pack}} \tag{2}$$

The packing energy is dominated by the electrostatic repulsion between neighboring semiflexible polyelectrolytes in liquid-crystalline condensates, and possibly enhanced by thermal undulations.[8,9] It can be estimated using theoretical equations of state for liquid crystalline semiflexible polyelectrolytes,[8,9] or computed from experimentally determined osmotic pressures of polyelectrolyte liquid crystals.[9] To estimate the amount of polymer needed to condense semiflexible polyelectrolytes, we use the fact that the chemical potentials, or insertion free energies, should be equal at the transition point:

$$f_{\text{ins,free}} \approx f_{\text{ins,cond}}. \tag{3}$$

To change the critical concentration of depletion agent needed for condensation (without changing the deplerion agent itself) requires changing either the insertion energy for free semiflexible polyelectrolytes, or the insertion free energy of condensed semiflexible polyelectrolytes. The former is especially sensitive to the radius a of the semiflexible polyelectrolyte, the latter especially to the polyelectrolyte linear charge density ν.

This is illustrated in Table 1 where we compare typical condensation thresholds for resp. naked DNA, Sso7d-coated DNA (saturated filaments), and F-actin filaments. The Sso7d protein is basic with an estimated charge at pH 7 of $+4 \cdots +6$ (extrapolated from Ref. 10). This means that the net electrostatic repulsion between saturated Sso7d-DNA filaments will certainly be less than that between naked DNA, but it is not clear by exactly how much.

Comparing with naked DNA and F-actin, it is clear that the increased effective polyelectrolyte radius induced by protein binding cannot fully explain the decrease of the condensation treshold. Therefore, it is very likely that in the present case, the decreased effective charge of the protein-DNA filaments also plays a significant role in reducing the condensation treshold.

Although we here assume flexible polymers as the depletion agent, the conclusions may be expected to hold more generally: thick protein-DNA filaments with a low net charge density are much more susceptible to depletion condensation, be it by flexible polymers, or by cytoplasmic, non-DNA binding proteins.

What is the role of this synergy in the formation and stabilization of nucleoids in prokaryotic cells? Odijk has convincingly shown[12] that for the supercoiled genomic DNA of bacteria, confined by the bacterial cell wall, depletion interactions of the DNA with non-binding proteins are sufficiently strong to drive a phase separation into a nucleoid phase rich in DNA (but not as concentrated as DNA condensates

Table 1. Critical polymer concentrations needed to condense semiflexible polyelectrolytes at ns = 0.15 M.

Polyelectrolyte	a (nm)	ν (enm)	w_c (%)
DNA	1.0 (Ref. 4)	0.17	8
Sso7d-coated DNA	2.5 (Ref. 4)		3
F-actin (Ref. 11)	4.0	0.25	3

obtained from dilute solutions) and a cytoplasm phase rich in non-binding globular proteins. Our results suggest that the effect of nucleoid proteins could be included in such a theory (to lowest order) by allowing for a somewhat larger thickness and a lower charge density of the DNA.

In any case, it is clear that if some particular nucleoid protein-DNA filament is extended and/or rigid in dilute solution, this clearly does not mean that the protein does not contribute to DNA compaction in the crowded environment of the living cell.

Acknowledgments

We thank Stephen Edmondson for providing the *E. coli* strain over-expressing Sso7d, and John van der Oost for useful discussions. E. Bessa Ramos was supported by CAPES grant 3515/04-4.

References

1. C. J. Dorman and P. Deighan, *Curr. Opin. Genet. Dev.* **13**, 179 (2003).
2. R. T. Dame and N. Goosen, *FEBS Lett.* **529**, 151 (2002)
3. J. van Noort, S. Verbrugge, N. Goosen, C. Dekker and R. T. Dame. *Proc. Natl. Acad. Sci. USA* **101**, 6969 (2004).
4. J. B. Krueger, B. S. McCrary, A. H.-J. Wang, J. W. Shriver, J. Trewhella and S. P. Edmondson, *Biochemistry* **38**, 10247 (1999)
5. L. D. Murphy and S. B. Zimmerman, *Biophys. Chem.* **57**, 71 (1995).
6. R. de Vries, *Biophys. J.* **80**, 1186 (2001).
7. J. G. McAfee, S. P. Edmondson, P. K. Datta, J. W. Shriver and R. Gupta, *Biochem.* **34**, 10063 (1995).
8. T. Odijk, *Biophys. Chem.* **46**, 69 (1993).
9. H. H. Strey, V. A. Parsegian and R. Podgornik, *Phys. Rev. E.* **59**, 999 (1999).
10. R. Todorova and R. Atanasov, *Int. J. Biol. Macromol.* **34**, 135 (2004).
11. J. X. Tang, T. Ito, T. Tao, P. Traub and P. A. Janmey, *Biochem.* **36**, 12600 (1997).
12. T. Odijk, *Biophys. Chem.* **73**, 23 (1998).

THE JOURNAL OF CHEMICAL PHYSICS 129, 185102 (2008)

Polymer induced condensation of DNA supercoils

José Ésio Bessa Ramos, Jr.,[1] João Ruggiero Neto,[1] and Renko de Vries[2,a)]
[1]*Department of Physics, IBILCE UNESP, Universidade Estadual Paulista, R. Cristóvão Colombo 2265, 15054-000 São José do Rio Preto SP, Brazil*
[2]*Laboratory of Physical Chemistry and Colloid Science, Wageningen University, P.O. Box 8038, 6700EK Wageningen, Netherlands*

(Received 20 May 2008; accepted 18 September 2008; published online 10 November 2008)

Macromolecular crowding is thought to be a significant factor driving DNA condensation in prokaryotic cells. Whereas DNA in prokaryotes is supercoiled, studies on crowding-induced DNA condensation have so far focused on linear DNA. Here we compare DNA condensation by poly(ethylene oxide) for supercoiled and linearized pUC18 plasmid DNA. It is found that supercoiling has only a limited influence on the critical amount of PEO needed to condense plasmid DNA. In order to pack DNA supercoils in condensates, it seems inevitable that they must be deformed in one way or another, to facilitate dense packing of DNA. Analytical estimates and Monte Carlo simulations indicate that packing of DNA supercoils in condensates is most likely facilitated by a decrease of the superhelical diameter rather than by unwinding of the supercoils.
 [DOI: 10.1063/1.2998521]

I. INTRODUCTION

Ever since its discovery by Lerman,[1] crowding-induced DNA condensation has been intensively studied as a model for DNA condensation in living cells, especially bacteria.[2,3] The physical mechanism behind crowding-induced DNA condensation is the general mechanism for phase separation in mixtures of asymmetric colloids: depletion interactions between the solution components.[4] In model studies the crowding agent usually is a flexible polymer [such as poly(ethylene oxide) or PEO] that is supposed to mimic high intracellular concentrations of globular proteins that do not bind to DNA. Recent experimental studies have focused on studying crowding-induced DNA condensation at the single-molecule level[5] and on re-entrant decondensation at low polymer molecular weight.[6] Recent theoretical studies have elucidated the strong ionic-strength dependence of the condensation treshold[7] and have shown that nonbinding globular proteins are, in fact, much poorer DNA-condensation agents than flexible polymers,[8,9] consistent with experimental observations.[10] Whereas DNA in these studies is invariable assumed to be linear, DNA in bacteria is typically circularly closed and supercoiled due to the twist introduced into the DNA by both specific enzymes and by processes such as transcription and replication.[11]

Supercoiled DNA inside prokaryotic nucleids is condensed to such an extent that it is not unreasonable to speculate that, in fact, it might exhibit liquid crystalline order,[3,12] and indeed there is some experimental evidence pointing in this direction.[13]

In contrast to the large number of studies on liquid-crystallinity of linear DNA,[14] only a few experimental papers have addressed the arrangement of supercoiled DNA in liquid crystalline condensed states.[15–17] These studies do suggest that the structure of individual plectonemic supercoils changes upon condensation. However, with the scattering methods used in these papers, it is difficult to separate scattering due to intersupercoil and intrasupercoil interferences. For this reason, scattering experiments provide only limited information on the conformational changes of individual DNA supercoils in the presence of a high concentration of surrounding DNA supercoils. Analytical estimates by Odijk[12] suggest that condensation and liquid-crystalline ordering could ultimately lead to supercoil unwinding but only in very strong nematic fields. Some earlier theoretical work[18] has addressed the issue how DNA topology influences the shape and packing of DNA in the toruslike condensates that form at very low DNA concentrations.

In this paper, we study how supercoiling affects crowding-induced DNA condensation, by comparing polymer-induced condensation of supercoiled and linearized plasmid DNA. A simple condensation assay is used to determine the critical amount of polymer needed to condense the DNA molecules. We find that there is little difference between the critical amounts of polymer needed to condense linear and supercoiled plasmid DNA. Apparently, supercoiling does not introduce a large free energy penalty for packing DNA into condensates. Since the supercoils are quite large and the condensate densities quite high, this means that there are low-energy supercoil deformations that facilitate packing. To elucidate the nature of the possible low-energy supercoil deformations, we develop analytical estimates for supercoil unwinding and use Monte Carlo simulations of a single DNA supercoil, mimicking the dense environment of surrounding supercoils through the use of a nematic field and an effective depletion attraction between DNA segments.

a)Electronic mail: renko.devries@wur.nl.

II. MATERIALS AND METHODS

A. Plasmid DNA

The plasmid pUC 18 was extracted from *E. coli* using a Qiagen Plasmid Mega Kit. The linearized form was obtained by enzymatic digestion (2 h at 37 °C) of the supercoiled DNA using the restriction enzyme EcoRI. The DNA concentration was measured spectrophotometrally (1.0 OD at 260 nm equals 50 μg/ml. of DNA). The ratio between A_{260}/A_{280} was found to be equal to 1.88; the integrity of both forms was checked using agarose gel electrophoresis (1% agarose).

B. Condensation assay

The condensation assay was similar to that used by Murphy and Zimmerman.[10] PEO (molar mass 20 kg/mol) was dissolved in 30 mM tris-HCl, *p*H 7.0 After that, the NaCl concentration was adjusted to the required value using a concentrated NaCl stock solution. 50 μl solutions of PEO were prepared at given concentrations (measured in wt %) of PEO and NaCl. As the last component, we added pUC18 (linearized or supercoiled) plasmid DNA, again from a concentrated stock solution, to a final DNA concentrations of 12 μg/ml. Solutions were left at rest for 1 h and centrifuged for 1 h at 14 000 g, at room temperature. A small aliquot (5 μl or 10% of the total volume of the solution) of the supernatant was collected immediately after centrifugation and its DNA content was analyzed using agarose gel electrophoresis (1% agarose). Images of the gels were analyzed using IMAGEJ software.

C. Monte Carlo simulations

Monte Carlo simulations of DNA supercoils were carried out as described previously,[19] except that a Verlet neighbor list was used to speed up the evaluation of the nonbonded interaction energies. In brief, a single, circularly closed, DNA molecule was modeled as a closed string of N beads at positions $\mathbf{r}_1 \cdots \mathbf{r}_N$ (with $\mathbf{r}_{N+1}=\mathbf{r}_1$), interacting through a Hamiltonian H that includes terms for bond stretching, bending energy, twisting energy, nonbonded interactions between the beads, and a term ΔH mimicking the influence of an environment consisting of neighboring densely packed DNA supercoils:

$$H[\mathbf{r}_1,\ldots,\mathbf{r}_N] = \frac{1}{2}k_s\sum_{i=1}^{N}(|\mathbf{r}_{i+1}-\mathbf{r}_i|-l_b)^2 + \frac{1}{2}k_b\sum_{i=1}^{N}\arccos(\mathbf{t}_i\cdot\mathbf{t}_{i+1})^2 + \frac{2\pi^2k_t}{N}(\Delta Lk - wr)^2 + \sum_{i=2,j<i}^{i=N}u(|\mathbf{r}_i-\mathbf{r}_j|) + \Delta H[\mathbf{r}_1,\ldots,\mathbf{r}_N]. \quad (1)$$

Unit tangents $\mathbf{t}_i$ are defined as $\mathbf{t}_i=(\mathbf{r}_{i+1}-\mathbf{r}_i)/|\mathbf{r}_{i+1}-\mathbf{r}_i|$, and k_s, k_b, and k_t are the elastic constants for, respectively, stretching, bending, and twisting. The equilibrium bond length for the beads is l_b, and ΔLk and wr are, respectively, the excess linking number and the writhe of the closed circular DNA. The isotropic potential of interaction $u(r)$ between the beads is taken to be a sum of steric repulsion and longer-ranged Debye–Hückel electrostatic repulsion,

$$\frac{u(r)}{kT} = \left(\frac{\sigma_d}{r}\right)^{12} + l_B\alpha^2\frac{\exp(-\kappa r)}{r}, \quad (2)$$

where σ_d is the DNA steric diameter, α is the strength of an effective Debye–Hückel point charge located in the center of the beads, $l_B=e^2/\varepsilon kT$ is the Bjerrum length, e is the elementary charge, ε is the solvent permittivity, and kT is the thermal energy. The Debye screening length of the electrostatic repulsion is $\kappa^{-1}=(8\pi l_B n_s)^{-1/2}$, where n_s is the number density of monovalent electrolyte.

The term ΔH is used to mimic the influence of an environment consisting of neighboring densely packed DNA supercoils on a single test DNA supercoil. We distinguish effective contributions at the one-segment and the two-segment level. At the one-segment level, the main effect is alignment and possible unwinding due to nematic ordering of surrounding DNA supercoils. This effect is taken into account through an effective nematic potential:

$$\Delta H_{\text{nem}}[\mathbf{r}_1,\ldots,\mathbf{r}_N] = \frac{1}{2}k_n\sum_{i=1}^{N}(1-(t_i\cdot\mathbf{n})^2),$$

where k_n is the strength of the nematic field, and $\mathbf{n}$ is the nematic director. The two-segment level corresponds to effective interactions between the two segments of the test DNA supercoil induced by an environment of neighboring densely packed supercoils. At this level, we believe that the main effect is an effective depletion attractions between test segments in the presence of high concentrations of surrounding DNA segments (see Sec. III),

$$\Delta H_{\text{depl}}[\mathbf{r}_1,\ldots,\mathbf{r}_N] = \sum_{i=2,j<i}^{N}u_{\text{depl}}(|\mathbf{r}_i-\mathbf{r}_j|).$$

The functional form of the depletion potential between beads that we have used here is similar to that used in our previous work on depletion attractions between DNA segments in the presence of nonadsorbing globular proteins:[9]

$$u_{\text{depl}}(r) = \begin{cases} v_{\text{depl}}(1-r/\xi), & r\leqslant\xi \\ 0, & r>\xi \end{cases}$$

for some value of the strength v_{depl} and range ξ of the depletion interaction.

Trial moves consisted of small random translations of randomly chosen beads. Trial moves were accepted or rejected based on the Metropolis Monte Carlo criterium. The stepsize of the moves was adjusted to give an acceptance ratio of about 50%. Parameter values were the same as in Ref. 19, and correspond to DNA bend and twist persistence lengths of, respectively, 50 nm and 75 nm, and an ionic strength of 0.15M.

From the saved trajectories, we determine the values of the writhe and diameter of the supercoils. The writhe is computed from the full Gauss integral for the polygon.[20] For the effective supercoil diameter, we first determine, for each (test) bead, the distance to the closest neighboring bead, ex-

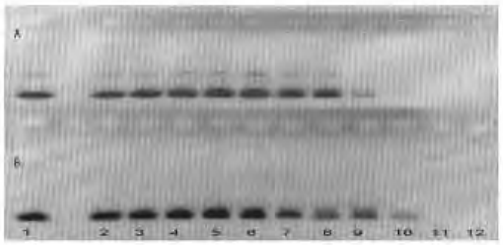

FIG. 1. Condensation assay. Mixtures with a fixed concentration of DNA and an increasing concentrations of PEO are centrifuged for 1 h at 14 000 g. The supernatant is analyzed with agarose gel electrophoresis. The figure shows typical gels for [NaCl]=0.15*M*. Lane 1: without PEO 20K; lanes 2–12: PEO 20K concentration increasing from 2 to 12 wt. %. (a) Supercoiled pUC 18, the faint band is a small amount of nicked DNA. (b) EcoRI linearized pUC18.

cluding 40 beads on the left and right sides of the test bead. The effective supercoil diameter reported is the average of these distances over all beads.

III. RESULTS AND DISCUSSION

A. Condensation assay

As can be seen in Fig. 1, the fraction of DNA in the supernatant after centrifugation starts decreasing at a PEO concentration close to 7% (w/v) at 0.15*M* of NaCl. Figure 2 shows the relative intensity of the bands for the supercoiled DNA and the corresponding linear form. As can be seen, the threshold concentration for condensation is nearly the same for both forms, the threshold for the supercoiled DNA being slightly higher than that of the linear DNA. Figure 3 shows the dependence of the critical PEO concentration as a function of the NaCl for both DNA topologies. The salt dependence is very similar for both DNA topologies, and is also very similar to the salt dependence that has been determined before for linear DNA using single-molecule fluorescence[5] and circular dichroism.[6]

B. Theoretical considerations

In previous theoretical work, we have shown that the critical concentration of flexible polymer needed to condense

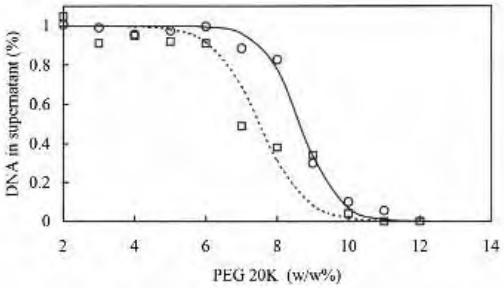

FIG. 2. Condensation assay. Intensity of the DNA bands as a function of wt % PEO 20K, again at [NaCl]=0.15*M*. Squares: EcoRI linearized pUC18. Circles: supercoiled pUC18.

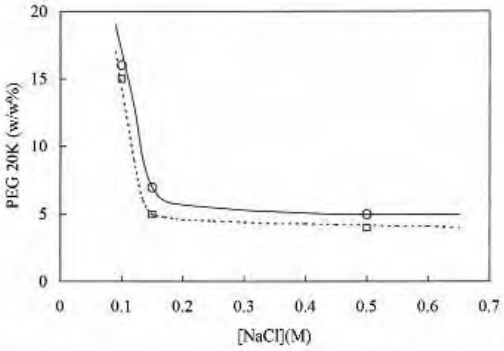

FIG. 3. Condensation treshold (PEO 20K wt % at which the intensity of the DNA bands in the condensation assay start decreasing) as a function of [NaCl]. Squares: EcoRI linearized pUC18. Circles: supercoiled pUC18.

DNA (assuming no flexible polymer is left in the condensates) can be estimated by equating the free energy of inserting DNA, respectively, in the free or condensed form in the polymer solution:

$$f_{\text{ins,free}} = f_{\text{ins,cond}}. \tag{1'}$$

Since generally the supercoil diameter is appreciably larger than the size or characteristic lengthscale of the crowding agent (in this case the correlation length of the semidilute PEO solution), the first term is expected to be essentially unaffected by DNA supercoiling, as was also argued previously by Odijk for the depletion of nonbinding globular proteins around supercoiled DNA.[3]

The second term $f_{\text{ins,cond}}$ might be increased by supercoiling (leading to a higher boundary for condensation) if it costs more to pack supercoiled DNA to the same density as linear DNA. Packing problems may be alleviated by deformations of the supercoils. The absence of a strong effect of supercoiling on the amount of polymer needed to condense DNA suggests that the free energy associated with these deformations is small, most likely appreciably smaller than the packing free energy itself.

In this section, we estimate the deformation energy associated with supercoil unwinding and compare it to the estimated packing energy, in order to see whether supercoil unwinding can qualify as a low-energy deformation that could facilitate the packing of DNA supercoils in a condensate.

For a typical plasmid superhelical density of $\sigma=-0.06$, the twisting energy per unit length of DNA for the completely unwound configuration is

$$\frac{H_{\text{twist}}}{L} = \frac{2\pi^2 CkT}{p^2}\sigma^2 \approx 0.4kT/\text{nm}, \tag{2'}$$

where $p=3.4$ nm is the equilibrium DNA helical pitch, $C=75$ nm is the DNA twist persistence length, and L is the DNA contour length. The actual energy required to completely unwrithe the supercoil to a flat configuration (with writhe $wr=0$) is less than this, since not all excess linking is stored as writhe: typically $wr/\Delta Lk \approx 0.6$. Hence a somewhat

sharper upperbound for the energy of completely unwrithing the supercoil is

$$\frac{H_{\text{twist}}}{L} \approx 0.24kT/\text{nm}. \tag{3}$$

Partial unwrithing and decreasing the superhelical diameter should only cost a fraction of this. In order to compare this deformation free energy to the actual packing free energy of the supercoils, we assume the latter is rather close to the free energy of packing linear DNA to the same density. If this were not the case, we would certainly have seen larger differences in the critical amount of polymer needed to condense the DNA. The free energy f_{pack} (per unit length) of packing linear DNA into a condensate is estimated according to the theory of Odijk[21] for hexagonally packed gels of semiflexible polyelectrolytes:

$$\frac{f_{\text{ins}}}{kT} = \frac{3(2\pi)^{1/2}\xi_{\text{eff}}^2}{l_B}\frac{\exp\left(-\kappa D + \frac{1}{2}(\kappa u)^2\right)}{\left(1+\frac{1}{2}\kappa u^2/D\right)} + \frac{c_{\text{und}}}{u^{2/3}P}, \tag{4}$$

where D is the lattice spacing, u is the rms amplitude of the thermal undulations of the semiflexible chains, ξ_{eff} is the effective dimensionless linear charge density of DNA (computed as in our previous work), and the numerical constant is $c_{\text{und}}=2^{-2/3}$. For a given lattice spacing D, the undulation amplitude u is determined by balancing the electrostatic repulsion (the first term, which favors small values of u) against the configurational entropy (the second term, which favors large values of u). We assume some typical numbers: a DNA center-to-center distance in the condensates of $D=6.5$ nm, an ionic strength $c_s=0.15M$, which gives a dimensionless DNA charge parameter of $\xi_{\text{eff}}=7.0$, and an undulation amplitude $u\approx 0.9$ nm. Under these conditions, the osmotic pressure is $\Pi=4.3\times10^4$ Pa, which corresponds to a PEO 20K concentration of about 7 wt %, close to the condensation threshold. For this case,

$$f_{\text{pack}} \approx 0.3kT/\text{nm}. \tag{5}$$

This is comparable to the free energy of completely unwinding the supercoils. Hence, significant unwinding is unlikely according to this estimate, since that would certainly lead to much higher packing energies and a higher boundary for condensation. Therefore, we should look for other low-energy deformations of the supercoils that could facilitate packing.

C. Monte Carlo simulations

Although we could also have developed estimates for other possible modes of deformation of DNA supercoils in condensates, such as a decrease of the superhelical radius, we instead decided to perform direct numerical simulations. Simulating a dense assembly of supercoils is at present too computationally intensive; therefore, we use a mean-field approach and simulate a single test supercoil under the influence of an averaged environment of surrounding supercoils. At the one-segment level, the main effect is nematic alignment, which has also been considered by Odijk.[12] We also consider the impact at the two-segment level: a dense environment of surrounding DNA supercoils will also influence interactions between two segments of the test supercoil.

1. Nematic fields

Following Odijk, we first consider the influence of a nematic field on configurations of plectonemic supercoils, where the nematic field is a simple approximation for the complex environment of nematic supercoils surrounding a certain test supercoil:

$$\Delta H_{\text{nem}}[\mathbf{r}(s)]/kT = \frac{1}{2}\Gamma P^{-1}\int_0^L ds[1-(\hat{\mathbf{n}}\cdot\hat{\mathbf{u}}(s))^2], \tag{6}$$

where $\hat{\mathbf{u}}(s)=\partial\mathbf{r}(s)/\partial s$ is the unit tangent along the continuous space curve $\mathbf{r}(s)$ describing the shape of the DNA of contour length L. The strength of the nematic coupling parameter Γ is related to the coupling strength k_n for the discrete DNA model used in the simulations by $\Gamma=k_nP/\langle l\rangle$, where $\langle l\rangle$ is the equilibrium bond length in the discrete DNA model (see Sec. II), and $P=50$ nm.

We simulated a small 1.3 kb DNA circle (corresponding to a contour length of about 450 nm) for two typical values of the superhelical density, $\sigma=-0.040$ and $\sigma=-0.055$, varying the strength of the nematic field from $\Gamma=0,\ldots,175$. For strong nematic fields, the orientational distribution is a Gaussian,

$$p(\theta) = \frac{\alpha}{4\pi}\exp\left(-\frac{1}{2}\alpha\theta^2\right), \tag{7}$$

where θ is the angle of the DNA axis with respect to the nematic director $\hat{\mathbf{n}}$. The constant α is related to the strength of the nematic potential by[12]

$$\Gamma = \tfrac{1}{4}\alpha^2. \tag{8}$$

From experimental data, Odijk[12] estimated that typically α does not increase much beyond O(10), implying that typically, $\Gamma<100$. Results for the superhelical diameter and the writhe from our simulations are shown in Fig. 4. At small field strengths, $\Gamma<30$, the supercoil responds by lowering its diameter. Only at very large field strengths, $\Gamma>30$, does the supercoil start unwinding (as shown by decreasing values of $wr/\Delta Lk$) at a relatively constant value of the superhelical diameter. Snapshots of typical configurations of the DNA supercoils without and with a (very strong) nematic field are shown in Fig. 5. The tentative upperbound of $\Gamma<100$ for DNA liquid crystals plus our simulation data indicate that a decrease of the superhelical diameter may certainly be expected, but that significant superhelical unwinding is unlikely consistent with the analyical estimates of the previous section and the estimates of Odijk.

2. Depletion attraction

The dense environment of supercoiled DNA not only tends to align individual DNA segments it also influences the effective interaction between two DNA segments of the test supercoil (for example, the interaction between segments on opposing sides of the plectonemic test supercoil). If we make a cut through the plane perpendicular to the nematic director, we have a two dimensional fluid of cross sections of DNA

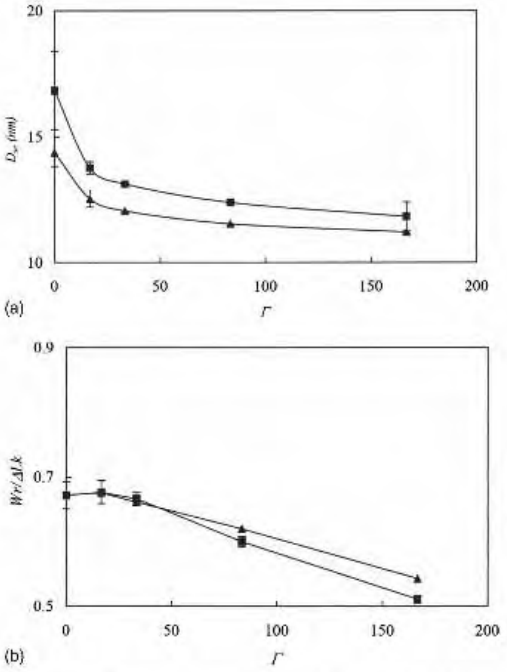

FIG. 4. Monte Carlo simulations of small 1.3 kb DNA circles in nematic fields, at two different superhelical densities: $\sigma=-0.040$ (squares) and $\sigma=-0.055$ (triangles). (a) Superhelical diameter D_{sc} as a function of the strength Γ of the nematic potential. (b) Writhe per added link $wr/\Delta Lk$ as a function of the strength Γ of the nematic potential.

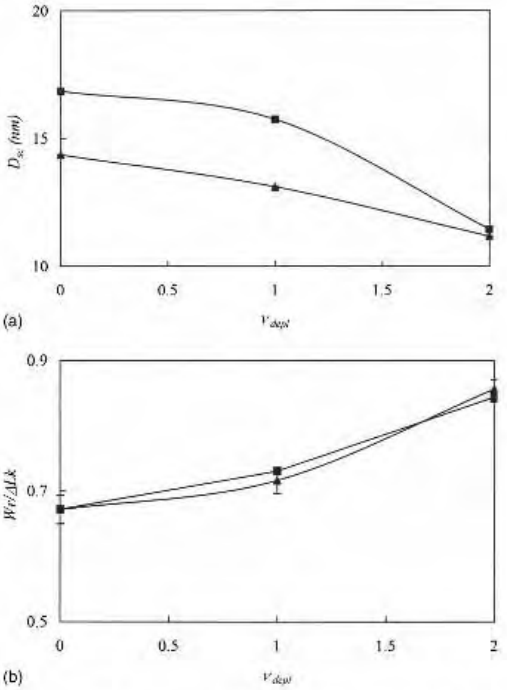

FIG. 6. Monte Carlo simulations of small 1.3 kb DNA circles with an added depletion attraction between the beads representing the DNA, at two different superhelical densities: $\sigma=-0.040$ (squares) and $\sigma=-0.055$ (triangles). (a) Superhelical diameter D_{sc} as a function of the strength v_{depl} of the depletion potential between the beads. (b) Writhe per added link $wr/\Delta Lk$ as a function of v_{depl}.

segments with a pair-correlation function $g(r)$ that we can interpret in terms of a potential of mean force $u_{mf}(r)$ between two nearly parallel DNA test segments,

$$g(r)=\exp(-u_{mf}(r)/kT). \tag{9}$$

This potential of mean force $u_{mf}(r)$ has a contribution $V(r)$ due to the direct interaction between nearly parallel DNA segments and a contribution $\Delta V(r)$ due to the presence of the large number of DNA segments surrounding the two test segments,

$$u_{mf}(r)=V(r)+\Delta V(r). \tag{10}$$

The potential $\Delta V(r)$ is effectively a depletion attraction: for distances shorter than some characteristic exclusion length ξ,

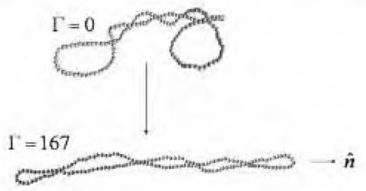

FIG. 5. Snapshot of typical configurations of the 1.3 kb DNA circles during the Monte Carlo simulations in the absence (top) and the presence (bottom) of a strong nematic field.

there will be no more DNA segment entering the space between the two test segments, and the test segments will be pushed together by the surrounding segments. For a crude estimate, we use the approach that we have previously used to estimate the depletion attraction between DNA segments (per unit length) induced by surrounding nonbinding globular proteins:[9]

$$\Delta V(r)=\begin{cases}-\frac{1}{2}f_{ins}(1-r/\xi), & r<\xi\\ 0, & r>\xi\end{cases}, \tag{11}$$

where in the present case, f_{ins} is the free energy per unit length of inserting a test segment in the liquid-crystalline suspension of DNA supercoils (i.e., the DNA chemical potential per unit length),

$$f_{ins}\approx\Pi(D)D^2. \tag{12}$$

This corresponds to a strength v_{depl} of the depletion attraction per bead as used in the simulations of

$$v_{depl}\approx\Pi(D)D^2\langle l\rangle=O(kT). \tag{13}$$

The exclusion range ξ is estimated as[9] $\xi\approx 2(\sigma_d+\kappa^{-1})\approx 6.5$ nm. Figure 6 shows the results for the superhelical diameter D_{sc} and for the writhe $wr/\Delta Lk$ as a function of the strength of the depletion potential. Not surprisingly, the

depletion attraction decreases the superhelical diameter, with the largest changes being observed for the most loose supercoils, with superhelical density $\sigma=-0.040$. Perhaps more surprising is that the attraction opposes unwinding of the supercoils, because the attraction brings the configurations closer to that of the optimal plectonemic supercoil in which all twists are relaxed into writhe and which has a superhelical diameter that tends to zero. This should be compared to the predicted dependence of $wr/\Delta Lk$ and D_{sc} on ionic strength that is found in the absence of depletion attraction:[22–24] longer ranged repulsion then leads to a lower $wr/\Delta Lk$ and a higher D_{sc}. Thus, increasing the attraction changes $wr/\Delta Lk$ and D_{sc} in the same way as decreasing the electrostatic repulsion (by lowering the ionic strength).

IV. CONCLUDING REMARKS

We have shown that depletion condensation of DNA induced by flexible polymers is hardly hindered by DNA supercoiling. This suggests that packing of supercoils must be facilitated by supercoil deformations that cost very little free energy. In agreement with the scaling estimates, the simulations show that significant unwinding of supercoils in the condensates is not very likely: This only occurs in very strong nematic fields and is opposed by effective depletion attractions operating between DNA segments in the condensates. The lowest energy deformation, promoted by both a nematic field and by depletion attraction, is a decrease of the superhelical diameter. This therefore seems to be the most likely candidate for the deformation that is necessary to pack DNA supercoils into condensates.

ACKNOWLEDGMENTS

We would like to thank Jan Verver and Joan Wellink for assistance with purifying and analyzing the DNA. E.B. was supported by a CAPES grant.

[1] L. S. Lerman, Proc. Natl. Acad. Sci. U.S.A. **68**, 1886 (1971).
[2] S. B. Zimmerman and L. D. Murphy, FEBS Lett. **390**, 245 (1996).
[3] T. Odijk, Biophys. Chem. **73**, 23 (1998).
[4] S. Asakura and F. Oosawa, J. Chem. Phys. **22**, 1255 (1954).
[5] V. V. Vasilevskaya, A. R. Khokhlov, Y. Matsuzawa, and K. Yoshikawa, J. Chem. Phys. **102**, 6595 (1995).
[6] J. E. B. Ramos, Jr., R. de Vries, and J. R. Neto, J. Phys. Chem. **109**, 23661 (2005).
[7] R. de Vries, Biophys. J. **80**, 1186 (2001).
[8] M. Castelnovo and W. M. Gelbart, Macromolecules **37**, 3510 (2004).
[9] R. de Vries, J. Chem. Phys. **125**, 014905 (2006).
[10] L. D. Murphy and S. B. Zimmerman, Biophys. Chem. **57**, 71 (1995).
[11] A. Bates and A. Maxwell, *DNA Topology*, 2nd edition (Oxford University Press, Oxford, 2005).
[12] T. Odijk, J. Chem. Phys. **105**, 1270 (1996).
[13] Z. Reich, Ellen J. Wachtel, and A. Minsky, Science **264**, 1460 (1994).
[14] F. Livolant and A. Leforestier, Prog. Polym. Sci. **21**, 1115 (1996).
[15] J. Torbet and E. Dicapua, EMBO J. **8**, 4351 (1989).
[16] Z. Reich, S. Levin-Zaidman, S. B. Gutman, T. Arad, and A. Minsky, Biochemistry **33**, 14177 (1994); S. Levin-Zaidman, Z. Reich, E. J. Wachtel, and A. Minsky, Biochemistry **35**, 2985 (1996).
[17] S. S. Zakharova, W. Jesse, C. Backendorf, and J. R. C. van der Maarel, Biophys. J. **83**, 1119 (2002).
[18] A. Yu. Grossberg and A. V. Zhestkov, J. Biomol. Struct. Dyn. **3**, 515 (1985).
[19] R. de Vries, J. Chem. Phys. **122**, 064905 (2005).
[20] K. Klenin and J. Langowski, Biopolymers **54**, 307 (2000).
[21] T. Odijk, Biophys. Chem. **46**, 69 (1993).
[22] A. Vologodskii and N. Cozarelli, Biopolymers **35**, 289 (1995).
[23] V. Rybenkov, A. V. Vologodskii, and N. R. Cozarelli, J. Mol. Biol. **267**, 299 (1997).
[24] J. Ubbink and T. Odijk, Biophys. J. **76**, 2502 (1999).

Flexible polymer-induced DNA condensation: Deviations from the scaling regime for flexible polymer solutions.

José Ésio Bessa Ramos Jr.
Physics Departament - Universidade Estadual Paulista -UNESP- Rua Cristovão Colombo 2365
CEP -15054000 – Jardim Nazareth - Campus de São José do Rio Preto – São Paulo - Brazil

Abstract

We address the theoretical problem of polymer-induced DNA condensation taking explicitly the polymeric nature of the depleting agent into account by solving the Edward's equation analytically. We also extend our model for flexible polymer solutions of low molecular weight for which the mean field Flory's theory seems to agree better with the experimental data than the scaling theory predictions. Our aim is to highlight the role of polymers molecular weight on the onset of the DNA condensation and reentrant decondensation. Some numerical results and comparisons with experimental data are presented as well.

Introduction

Under certain physical-chemical conditions, DNA molecules may aggregate or condense without precipitating out of the solution. A specific case is the one in which a flexible polymer is added to a DNA solution at a given ionic strength [1]: if the DNA solution is dilute and the DNA molecules are long enough (~10^5 base pairs), a mono-molecular collapse will occur[2]; on the other hand, if the solution is concentrated and the DNA molecules are shorter (~10^3 base pairs) multi-molecular collapse or aggregation most likely will take place[3,4].In both cases, depletion interactions between the polyelectrolyte segments and the flexible polymer coils are the general physical mechanism underlying the DNA condensation/aggregation: the flexible chains are depleted from the surroundings of the DNA segments and as soon as the depletions layers do overlap an attractive potential between the DNA segments arises[5].

The **psi-**condensation (**p**olymer and **s**alt-**i**nduced or **ψ**-condensation as is known the aforementioned DNA-flexible polymer phase separation) has been studied intensively both theoretical and experientially since the DNA condensate itself is important as a simplified model for the DNA organization in virus and prokaryotic living cells and moreover, the intricate interactions taking place in solution may improve our basic knowledge about semi-flexible (charged)/flexible chains interactions and its phase behavior. However, in some specific conditions under which **ψ**-condensation is observed experimentally there is until now a lack *of formal consistency* for the *physical causes* invoked to explain the phenomenon has not being incorporated within the theoretical framework namely, *depletion of the flexible polymer molecules* from the space in between the interacting segments, particularly for short flexible polymer chains (polymers of low molecular weight) at high enough concentrations (semi-dilute regime).

Some theoretical works published so far explicitly account for the liquid-crystalline nature of the DNA condensates (which is experimentally known) and for the strong electrostatic repulsion among them as well,[6] describing the phase diagram (*i.e.*, the amount of flexible polymer needed to induce the ψ-condensation as a function of the solution ionic strength) accurately under the assumption that the flexible polymer is totally excluded from the DNA condensate, which is true if the flexible polymer is large enough (see discussion). Other theoretical works do account for an imperfect phase separation between the polyelectrolyte and the depleting agent neglecting both the liquid-crystalline state of the DNA molecules and the polymer's reduced configuration space inside the condensed phase and so the *partitioning* of the flexible polymer coils between the condensate and the solution [7, 8] which is regarded as the physical source of the attractive interaction among the polyelectrolyte segments [5]. Moreover, no attempts to account for deviations from the scaling predictions for the thermodynamic properties of flexible polymer solutions have been done so far. Since the predicted universal behavior is bounded by large degree of polymerization, it would be worthwhile to consider the general case of any polymer molecular weight.

The purpose of the present paper is therefore two fold: first to account explicitly for the

polymeric nature of the depleting agent and in doing so, treat more realistically the DNA-flexible polymer interaction which drives the phase separation; and second to account for the deviations from the scaling regime when the flexible polymer chains are small enough and the mean field theory for polymer solutions (Flory-Huygens theory) is expected to be fulfilled.

In the next section, we will describe the system to be studied and discuss the analytical approximations used to that; next using some tools from polymer physics and the principles of equilibrium thermodynamics we will show some numerical results. In doing so, we are presenting a more general theory for the phase separation between polyelectrolytes and flexible polymers which does not suffer from the restrictions of the previous ones and may have some practical applications as well.

Theory

1-Defining the system

The definition of the system to be studied is given below and its most important components described along with the approximations involved (see figure 1):

A semi-flexible polymer chain carrying a net electrical charge, i.e. a polyelectrolyte (DNA in the specific case of this work) which is assumed to be a completely rigid cylinder at the length scale of its persistence length (L_p=50 nm assumed to be constant on the entire salt concentration range) is dissolved in a water-salt solution (monovalent salt) along with a flexible polymer molecules. Each polymer chain has N monomers with an excluded volume l_k^3 per segment. Deviations from the thermodynamic scaling regime (strictly valid for $N\rightarrow\infty$) are accounted by empirical corrections in the scaling exponents. The solvent's quality for the flexible polymer is assumed to be good (and so the excluded volume effects are fully present) and its concentration regime is assumed to be dilute or semi-dilute.

The most relevant interactions in the system described above are assumed to be:

1) The DNA-DNA excluded volume interaction enhanced by the strong electrostatic repulsion which is included along the lines of Odijk's theory for excluded volume between polyelectrolytes [9]. In this theory, the effective DNA-DNA excluded volume per segment is decomposed in an intrinsic component (independent of the medium composition) and in an electrostatic component depending on the ionic strength; 2) The DNA-flexible polymer interaction which explicitly accounts for the polymeric nature of the depleting agent. A "cell model" (see figure 2) is used to describe the confinement of the flexible chain among the DNA segments and the Edward's equation is used to estimate the confinement energy of the polymer coils within a cylindrical cell [10](note that here we are following closely the pioneering work of Asakura and Oosawa about depletion interactions). The thermodynamic quantities of interest (such as osmotic pressure and chemical potential) are evaluated explicitly (see figure 2); 3) the flexible polymer interactions which are important especially in the semi-dilute regime and which has shown to influence the phase behavior of colloidal mixtures [7].

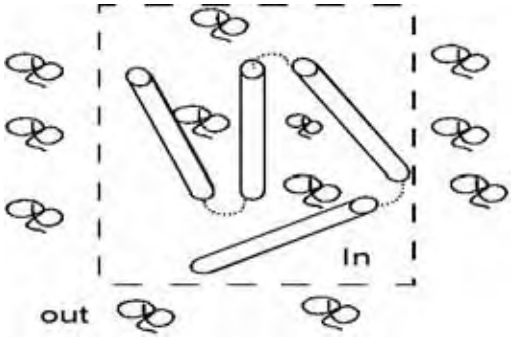

Figure 1-Picture describing the main components of the DNA-flexible polymer solution. The DNA segments are represented by the cylinders and are connected by the dotted lines. The flexible chains are represented by small coils. The dashed rectangle delimits the region occupied by the DNA molecule and is in contact with a flexible polymer reservoir.

2- Analytical approximations.

In order to describe the interaction between the DNA and the flexible polymer, we will use a “cell model” description. Figure 2 depicts the parameters involved in this approach. We consider a cell which totally encloses one DNA Kuhn segment and the flexible-polymer chain and analyze locally the DNA-flexible polymer interaction.

The following simplifying assumptions have been used to solve the Edward's equation (as discussed above): 1) The cell has a cylindrical symmetry and is infinity along the *z*-axis and 2) additionally, we assume that the monomers are not adsorbed at the DNA surface (“reflecting walls”). Our aim is to solve the Edward's equation:

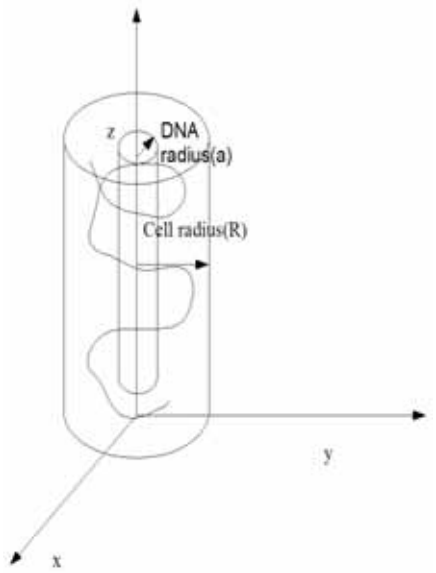

Figure 2- Schematic picture of a “cell” which encloses one DNA segment and the flexible chain. The central axis of the DNA segment (the DNA radius is represented by *a*) coincides with the *z*-axis and the flexible chain is represent by the continuous curve (coil-like conformation) around the DNA central segment. The cell has its radius represented by *R* where the axes of the neighboring segments are located (not represented for the sake of clarity).

$$l_k^2/6 \ \blacksquare_r^2 G(\boldsymbol{r},\boldsymbol{r_o},\boldsymbol{N}) + V(\boldsymbol{r})G(\boldsymbol{r},\boldsymbol{r_o},\boldsymbol{N}) /K_BT = \partial_N G(\boldsymbol{r},\boldsymbol{r_o},\boldsymbol{N}) \qquad (1)$$

In the equation 1, the Laplacian operator $\blacksquare_r^2$ acts on the Green's function G which represents the probability density distribution function for the *chain endpoints* $\boldsymbol{r}$ and $\boldsymbol{r_o}$; the chain has N monomers and ∂_N represents the partial derivative of G with respect to N. The potential energy of a monomer at a position $\boldsymbol{r}$ is represented by $V(\boldsymbol{r})$.The absolute temperature is represented by T and K_B represents the Boltzmann's constant. The Kuhn segment is represented by l_k.

Equation 1 may be solved by the method of separation of variables and the spatial solution written as bilinear series. Here we limit the discussion to the solution of that equation with the boundary conditions which must be satisfied by the physical problem: $G(\boldsymbol{r},\boldsymbol{r_o},\boldsymbol{N})$ must vanish at the surface of the DNA central segment ($r = a$) and at the border of the cell ($r=R$) we must have an extrema or an inflexion point for the local monomers concentration. We also neglect any dependency on the angular coordinate and end effects of the DNA segments (cylindrical symmetry).Thus the solution (un-normalized) may be written as:

$$G(\boldsymbol{r},\boldsymbol{r_o},N) = (AJ_o(Kr_o)+BN_o(Kr_o))(AJ_o(Kr)+BN_o(Kr))\ exp(-K^2l_k^2/N) \qquad (2)$$

and the following equations must be satisfied (boundary conditions):

$$AJ_o(Ka)+BN_o(Ka)=0 \qquad (3)$$

$$\partial_r\,(AJ_o(Kr)+BN_o(Kr))=0 \quad \text{at} \quad r = R \qquad (4)$$

Equations number 3 and 4 must be solved simultaneously for the ratio A/B (A and B are the integration constants required by the solution of an ordinary differential equation of second order) and K is the separation constant. Therefore the following equality must be satisfied:

$$J_o(Ka)N_1(K\,R) - N_o(Ka)J_1(K\,R)=0 \qquad (5)$$

In the equations above, J_0 and N_0 are the non modified Bessel's functions of first and second kind respectively and zero order, and J_1 and N_1 are the non modified Bessel's equations of first and second kind respectively and first order [11]. The constant *K* has to be evaluated numerically from equation 5. Within a certain limited range of values for *R,* we may approximate *K* (nm^{-1}) as a functions of $(R\text{-}2a)^{-1}$ (nm^{-1}).

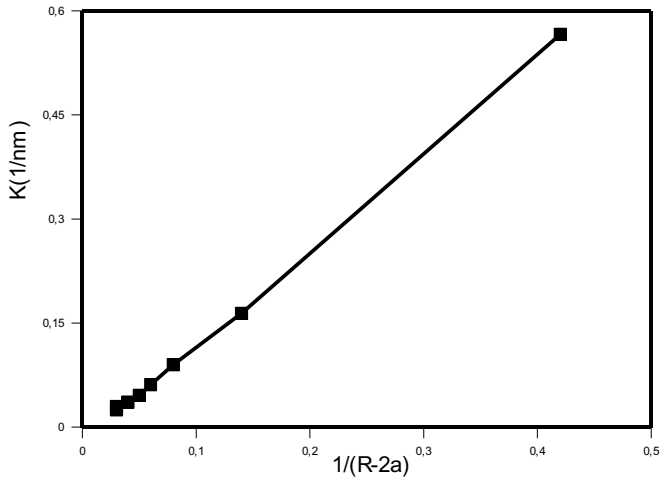

Figure 2- $K(nm^{-1})$ (the solution of equation 5) as a function of 1/(R-2a) (nm^{-1}) within a limited range of R values.

The partition function is given by [10]:

$$Z = \iint G(\boldsymbol{r},\boldsymbol{r_o},N)\, 4\pi^2\, d\boldsymbol{r}\, d\boldsymbol{r_o} = exp(-K^2 l^2_k/N) \qquad (6)$$

being the integrals performed over the spatial coordinates whose limits of integration are *a* and *R* (*r* and r_o specifying the position of both ends of the confined chain). Thus, we are just selecting those chain conformations (among all conformations available to the chain in the bulk of the solution) whose the end-to-end vector satisfies the boundary conditions (equation 5).
Since the free energy of the system is given by:

$$\Delta F = - K_B T \ln Z \qquad (7)$$

being Z is the partition function of the system, the free energy of confinement (*i.e.*, the interaction between the DNA and the flexible polymer is given by):

$$\Delta F = - K_B T \ln Z = c^2 K_B T R_g^2 / (R-2a)^2 \qquad (8)$$

being R_g the radius of gyration of the flexible polymer and c a constant estimated from the slope of the figure 2($c \approx 1.2$). Once we know the free energy of confinement, we can get the chemical potential and the osmotic pressure contributions due to confinement taking the derivative ΔF with respect to the number of molecules and the cells volume respectively:

$$\mu_{conf} = c^2 K_B T R_g^2 / (R-2a)^2 \qquad (9)$$

and

$$\Pi_{conf} = \Phi\, c^2 K_B T R_g^2 / N l_k^3 (R-2a)^2 \qquad (10)$$

being Φ the polymer volume fraction confined between the DNA segments.

2.2- The interaction between the flexible polymer chains.

Here we will assume that the concentration of the flexible polymer may be diluted or semi-diluted and use the following interpolating equation to describe the osmotic pressure in the entire concentration range:

$$\Pi_{osm} = K_B T \Phi / (N l_k^3) + K_B T a \Phi^b \qquad (11)$$

where Φ is the volume fraction of the polymer in solution, N is the number of monomers per chain and l_k^3 is the volume of one monomer; a and b are coefficients determined from the experimental measurement of the osmotic pressure (for polymers of high enough molecular weight we can use the scaling predictions). The first term in the equation 11 represents the ideal term (van't Hoff term) and the second term contains the interaction between the polymers chains.

The chemical potential is determined from the osmotic pressure and is written as:

$$\mu_{conf} = \mu_o + K_B T \ln \Phi + a\, b\, K_B T\, N\, l_k^3\, \Phi^{b-1} / (b-1) \qquad (12)$$

being μ_0 is the chemical potential of the polymer in the pure state, the second term is the ideal chemical potential and the last term is the excess of chemical potential *i.e.*, the change in free energy per polymer molecule due to the change of the solution volume from “infinity” to a finite value keeping the total number of polymers molecules constant [12].

2.3 – The interaction between the DNA segments.

Now we need describe the interaction between the DNA molecules and its contribution to the pressure inside the condensate. A rigorous equation of state for liquid crystalline DNA has

been formulated by Odijk [13]. However here we will adopt a simpler approach which allows an estimation of the pressure inside the condensate due do the DNA segments interactions. It is written as the first term of a virial expansion in terms of the numerical DNA segment density [7]:

$$\Pi_{DNA} = K_B T \beta c^2_{DNA}/2 \qquad (13)$$

where c_{DNA} is the numerical concentration of DNA Kuhn segments of length L_k= 100 nm and radius a_{bare}=1.2nm . The parameter β is the excluded volume from one DNA segment by another and is equal to $\pi L_k^2 a_{bare}/2$.

In agreement with X-ray diffraction measurements we will assume that the arrangement of the DNA segments inside the condensate is hexagonal and so the numerical concentration of DNA Kuhn segments is given by $c_{DNA} \approx 1.15x10^{-2}/R^2$ being R the inter axial DNA distance. The exact arrangement of the neighboring DNA segments must not be so important for macroscopic quantities otherwise local properties such as the monomer concentration profile along the cell's radial coordinate. Since we are interested in the former, this is not a so strong assumption which indeed is confirmed *a posteriori*.

The salt dependence is included along the lines of the Odijk's theory [9] for the excluded volume interactions between polyelectrolyte: we may assume an effective DNA radius as a function of the ionic strength thus accounting for the electrostatic contribution to the excluded volume among the DNA segments (neglecting any dependence of its persistence length on the ionic strength):

$$a_{eff} = a_{bare} + \kappa^{-1}(n_s) \qquad (14)$$

In equation 14 a_{bare} represents the DNA radius (~ 1.2 *nm*) and κ^{-1} is the Debye length which may be approximated at room temperature (298 *K*) by $0.3/n_s^{½}$ being n_s the monovalent salt concentration in molar units.

3- Results and discussion

As already mentioned the flexible polymer confinement among the DNA segments is the source of the effective attraction which ultimately leads to the phase separation: due to the loss of entropy the flexible polymer is partitioned between the two phases (see figure 1) and the unbalanced osmotic pressure push the polyelectrolyte segments together. Figure 3 shows the change in the free energy (the entropy change, essentially) of the flexible polymer as a function of the DNA inter axial distance for different degrees of polymerization (or different radii of gyration) for a polymer typically used in experiments, poly (ethylene oxide) or PEO or yet poly (ethylene glycol) or PEG.It is clear that small polymer coils may enter the condensate without a high free energy cost rather then the large ones or in other worlds the

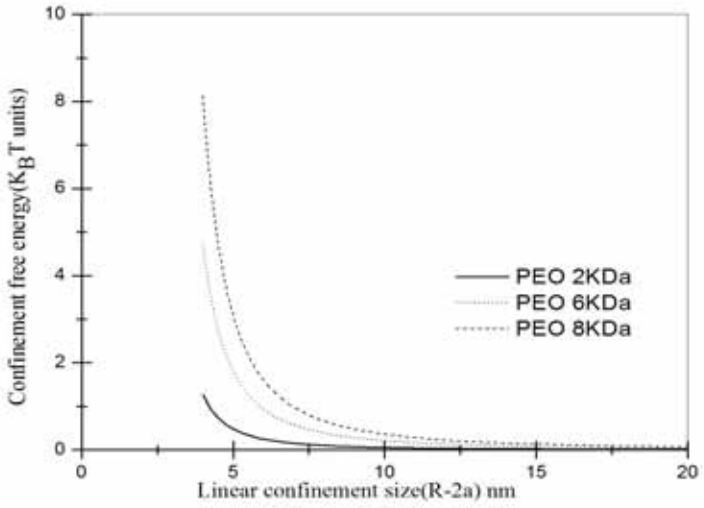

Figure 3- Confinement free energy (K_BT units) as a function of the cell's confinement dimensions R -2a (*nm*) for PEO 2k, 6k and 8k (R_g=1.5, 2.7 and 3.8 nm) . The values of R_g were taken from reference 15.

partition coefficient decreases with the increase of polymers molecular weight. Therefore the assumption of total exclusion of PEO coils from the condensates is justifiable on theoretical grounds and is in agreement with the de Vries theory for polymer-induced DNA condensation [6]. The present theory however aims at the opposite case in which the polymer coils are small enough to enter the condensed phase and thus contribute to the osmotic balance.

Therefore, in order to describe the phase equilibrium (or to locate the free energy minima of our system) we need to impose the equality of 1) the chemical potential μ of all species in both phases (in the figure 1 these phases are represented by "in" and "out") and 2) the equality of the osmotic pressure Π_{osm} in both phases [14]. Thus, the following equations must be satisfied:

$$\mu_{ins} = \mu_{out} \quad (15)$$

$$\Pi_{ins} = \Pi_{out} \quad (16)$$

The equations number 9 and 12 give us the equality of the chemical potential (both inside (*ins)* and outside (*out*) the globule) and the equations number 11 and 13 give us the equality of the osmotic pressures represented by equations number 16 and 17 respectively:

$$ln\ \Phi_{out} + a\ b\ N\ l_k^3 \Phi_{out}^{b-1}/(b\text{-}1) = ln\ \Phi_{ins} + a\ b\ N\ l_k^3\ \Phi_{ins}^{b-1}/(b\text{-}1) + c^2\ R_g^2/(R\text{-}2a)^2 \quad (17)$$

$$\Phi_{out}/(\mathrm{N}\ l_k^3) + K_B T a\ \Phi_{out}^{\ b} = \Phi_{ins}/(\mathrm{N}\ l_k^3) + a\ \Phi_{ins}^{\ b} + \beta c^2_{DNA}/2 \quad (18)$$

Next, we will discuss some numerical calculations for specific values of the microscopic parameters of the flexible polymer PEO: N (number of monomer per flexible chain), l_k^3 (excluded volume per segment), R_g (radius of gyration of the flexible polymer) [15], a_{eff} (DNA effective radius) and for specific values of the empirical parameter a and b which are known to deviate from the scaling predictions ($a = K_B T/l_k^3$ and b=9/4) for low enough molecular weight. Here we use the measurements of the osmotic pressure (web site) [16] to estimate these coefficients. Table 1 shows the values used in our numerical calculations and from them we may conclude that for PEO 2k the Flory's theory for polymer solution (which predicts an exponent *2* for the semi-dilute regime) is in better agreement with the experimental data in the concentration range 10-30% (volume fraction %) than the scaling predictions, the latter being attained for PEO 8k. These corrections may be relevant to draw even qualitative conclusions at such concentrations since we expect that the interactions among the flexible polymers coils increases with its molecular weight.

PE0	a	b	R_g(nm)	N	$l_{k(nm)}$
2k	16±0.8	2.05±0.05	1.5	45	0.4
8k	18.5±0.5	2.23±0.03	3.8	182	0.4

Table 1- Coefficients obtained from the osmotic pressure measurements of PEO 2k and 8k in the concentration range 10-30% and the respective microscopic parameters.

The polymer volume fraction in the outer phase (Φout) is imposed and the polymer volume fraction in the inner phase (Φ_{in}) and the distance between the DNA strands (R) are dependent variables. Figure 3 shows the dependence of the DNA segment concentration (c_{DNA}) as a function of the flexible-polymer volume fraction for PEO.

It is clear that the DNA segment density "inside the cell" changes discontinuously (or "jumps") from its coil density (nearly zero) to a higher value at some PEO concentration which we identify as the onset of the DNA condensation: the depletion interactions between

DNA segments and the PEO coils overcome the DNA-DNA repulsive interactions and the molecule collapse. The critical amounts of PEO *depend* on the *coil sizes* as expected: the range scale of depletion interactions depends on the sizes of the depleted solutes *i.e*., the polymer critical amounts decrease as R_g increases (see fig 3). In particular, we have also found that for very small PEO coils (R_g< 1 nm) there is no condensation at all *i.e*., the small coils may enter the condensate mostly without any hindrance and so there is no polymer partitioning between the condensed phase and the solution. Both facts have been verified experimentally [3].

Increasing the PEO concentration leads to a monotonic increase in the DNA numerical segment density. However at some higher PEO concentrations the DNA segment density returns to its coil density. This may be explained as follow: in the semi-dilute the interaction among PEO coils becomes more and more important (in contrast with the dilute regime in which each coil is to some extend isolated from the others); above a certain concentration (Φ* or overlap concentration) the important length scale for the DNA-polymer interaction is not the polymer radius of gyration (R_g) but rather the correlation length (ξ) of the PEO solution which decreases as its polymer volume fraction increases ($\xi \sim \Phi^{-3/4}$) [17]. The decrease in ξ leads to a decrease in the depletion potential and at some higher PEO volume fraction, the repulsive DNA-DNA interactions may overcome the polymer-induced attraction: the DNA condensate returns to its disperse form.

The reverse transition is known as reentrant decondensation and has been experientially observed as well [2, 3]. Note that the PEO critical amounts for reentrant decondensation also depend on the coils size: small PEO coils within the condensate contribute to the osmotic balance favoring the resolubilization in contrast with the large ones which are somewhat excluded from the condensed phase. These aspects are also in agreement with the experimental findings [3].

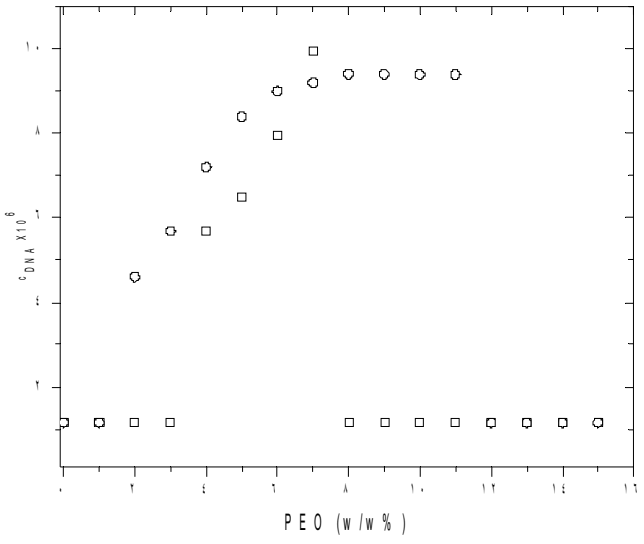

Figure 4- DNA numerical segment concentration c_{DNA} (nm^{-3}) as a function of the PEO concentration (in weight % - w/w%) for N = 45 (PEO 2k represented by squares) and N=182 (PEO 8k represented by circles).The ionic strength is fixed at 0.3M of a monovalent salt (*e.g*, NaCl). Around 5% and 2% of PEO 2k and 8k the DNA coil collapse (DNA condensation) which resembles a first-order transition and its density increases with the PEO concentration. At around 8 % and 12% of PEO 2k and 8k respectively the DNA condensate returns to its disperse state in solution (DNA reentrant decondensation) discontinuously which also resembles a first-order transition.

4-Concluding remarks

Throughout this work, we have tried to show how to overcome inherent limitations of previous theories of polymer-induced DNA condensation, specially concerning the polymeric nature of the depleting agent which has been explicitly accounted by this work and deviations from the scaling regime which is hardly attained in the actual experiments and may lead us to overestimate the interaction among small flexible polymer coils. The partitioning of the polymer among the polyelectrolyte segments and the bulk of the solution as well as the measured interaction among PEO coils (the osmotic pressure measurements) are accounted explicitly to highlight the role of the PEO molecular weight in the phase behavior of the DNA/PEO mixtures. It is also clear that the DNA electrostatic interactions are underestimated since we use the simplest way to account for that. A detailed treatment of the DNA-DNA has been given by Odijk [13] and is shown to correctly describe the strong salt dependence of the critical amounts of flexible polymers by de Vries [6].Since our goal here is just to point out the role of deviations from the scaling predictions in the DNA-flexible polymer condensation rather than draw a precise phase diagram, equation 13 seems a reasonable choice as a first approximation.

References

1- L. S. Lerman, *Proc. Natl. Acad. Sci*. **1971**,(68):1886-1890

2-V.V.Vasilevskaya., A.R.Khokholov.,Y.Matsuzawa, and H.Yoshikawa, *The J. Phys. Chem. B*. **1995**,(102):6595-6661

3- J. E.B. Ramos, Jr, R de Vries, and J. R. Neto, *The J. Phys. Chem. B*. **2005**,(236):67-70

4- G. Kleideter and E. Nordmeir. *Polymers*. **1999**, (40): 4025-4031

5- S. Asakura and F. Oosawa. *J. Phy. Chem*. **1954**, (22):1225-1226

6- R. de Vries. *Biophy J*. **2001**,(80): 1186-1194

7- M. Castelnovo and W. M. Gelbart. *Macromolecules*. **2004**, (37): 3510-3517

8- A. Yu. Grosberg, I. Ya. Erukhinovitsh, and E. I. Shakhnovitch. *Biopolymers*. **1982,** (21): 2413-2432

9- T. Odijk. *J Poly.Sci*. **1978**, (16):627-639

10-M. Doi and S.F. Edwards-*The Theory of Polymers Dynamics*- Clarendon Press, Oxford. **Chapter 2.**

11- G.N. Watson – *Theory of Bessel functions* – Cambridge University Press -**1922**

12-I.Teraoka- *Polymer Solutions: An introduction to physical properties*. John Wiley and Sons,

Inc. **2002**.
13-T. Odijk. *Biophys. Chem*. **1993**, (46): 69-75
14-L. D. Landau and E.M Lifshitz- **Volume 5** of *Course of theoretical physics* - **Part 1-Chapter VIII** Pergamon Press -Third Edition.
15-N.L.Abbot., D. Blankschtein, T.A. Hatton. *Macromolecules*. **1992**, (25-3): 3932- 3841
16 -Web-Site: www.brocku.ca/researchers/peter_rand/osmotic/osfile.html. (04/2009)
17-P. G. de Gennes – *Scaling Concepts in Polymer Physics*- Cornell University Press, Ithaca- **1979**.